

https://dspace.org/

Sedimentation tempo in an Early Jurassic erg system Refined chronostratigraphy and provenance of the Clarens Formation of southern Africa

H.V Head; E.M Bordy; Robert Bolhar

WILEY-BLACKWELL
https://hdl.handle.net/10539/40925
WOS

Downloaded from a DSpace repository. https://dspace.org/

Check for updates

Received: 30 July 2023 | Revised: 8 May 2024 | Accepted: 24 May 2024

DOI: 10.1111/bre.12877

Basin Research IAS EAGE WILEY

RESEARCH ARTICLE

Sedimentation tempo in an Early Jurassic erg system: Refined chronostratigraphy and provenance of the Clarens Formation of southern Africa

Howard V. Head[1] | **Emese M. Bordy**[1] | **Robert Bolhar**[2]

[1]Department of Geological Sciences, University of Cape Town, Rondebosch, South Africa

[2]School of Geosciences, University of the Witwatersrand, Johannesburg, South Africa

Correspondence
Howard V. Head, Department of Geological Sciences, University of Cape Town, Rondebosch 7701, South Africa.
Email: hvhead@gmail.com

Funding information
Genus; South Africa's National Research Foundation; PAST Africa; Society for Sedimentary Geology; Geological Society of America; Geological Society of South Africa

Abstract

The Clarens Formation is a widespread aeolianite deposited over southern Gondwana and represents the final phase of erg evolution in the main Karoo Basin during the Early Jurassic. Previous age assessments of the formation hinge on limited detrital zircon data, supplemented by relative ages from the biostratigraphy and geochronology of the adjacent Karoo units. This study refines the depositional history of the Clarens Formation, including its sediment source dynamics as well as basin-wide geochronological framework, based on U–Pb dating of detrital zircon grains, together with petrographic and sedimentological characterization. The abundant presence of heavy minerals like zircon, tourmaline and rutile suggests large-scale detritus recycling, while the uniform sandstone composition on a regional scale is an indication of sediment homogenisation across the basin. Based on the prominent detrital zircon age fractions, the sediments are interpreted as having been reworked from pre-existing rocks of the Karoo Supergroup (Permian), the Damara and Saldania Orogenic belts (650–490 Ma), whereas minor sources can be assigned to the Namaqua-Natal Mobile Belt (1.35–1.1 Ga) and the western Sierras Pampeanas (1.30–1.33 Ga). Unstable minerals (hornblende, garnet, titanite, feldspar) provide evidence for a nearby granitic source east and southeast of the basin, related to likely Grenvillian rocks (1.0–1.3 Ga). An Early Jurassic zircon age fraction is linked to volcanic activity in the Chon Aike Magmatic Province that, at the time, was situated south and southwest of the study area. Maximum depositional ages derived from these detrital zircon dates suggest that the sedimentation of the Clarens Formation spanned an interval of ~10 Ma during the Pliensbachian and early Toarcian. More specifically, the lower part of the formation is of early Pliensbachian age or younger (~191–192), while the upper part is of early Toarcian age or younger (~181–183 Ma). These age patterns are particularly prominent in the south of the basin that was situated closer to the volcanic source.

KEYWORDS

Aeolian systems, Clarens Formation, Early Jurassic, U–Pb detrital zircon geochronology

This is an open access article under the terms of the Creative Commons Attribution License, which permits use, distribution and reproduction in any medium, provided the original work is properly cited.
© 2024 The Author(s). *Basin Research* published by International Association of Sedimentologists and European Association of Geoscientists and Engineers and John Wiley & Sons Ltd.

2 | INTRODUCTION

In recent years, the application of detrital zircon U–Pb geochronology has emerged as a valuable tool for not only constraining the age of clastic deposits but also elucidating their provenance and resolving the dynamics of the host sedimentary basins, including the spatio-temporal evolution of the sediment supply mechanisms (Bertolini et al., 2020; Dickinson & Gehrels, 2003, 2009; Muhs, 2004; Muir et al., 2020). Several authors have applied this technique to resolving source dynamics and age constraints for ancient aeolian sedimentary systems (e.g., Bertolini et al., 2020; Dickinson & Gehrels, 2003; Gehrels et al., 2020; Zieger et al., 2020). Aeolian systems are generally associated with compositionally and texturally mature sediments, dominated by homogenous, quartz-rich, sand-size particles. During the Early Jurassic, extensive aeolian deposits were distributed across Pangea (Figure 1a; Blakey et al., 1988; Dickinson & Gehrels, 2003; Hasiotis et al., 2021; Kocurek & Dott, 1983; Loope et al., 2004; Rodríguez-López et al., 2014; Scherer & Goldberg, 2010; Scherer & Lavina, 2005; Scherer et al., 2007), and remnants of this vast ancient desert system can be found across southern Africa, preserved in the upper part of the Karoo Supergroup. This clastic sedimentary succession (Figure 1b) accumulated from the Late Carboniferous to the late Early Jurassic and corresponds to the assembly and breakup of Gondwana, respectively (Catuneanu et al., 1998, 2005; Muir et al., 2020).

In the main Karoo Basin (MKB; Figure 1), the Lower Jurassic aeolian deposits are exemplified by the Clarens Formation (Beukes, 1969, 1970; Bordy & Head, 2018; du Toit, 1905; Eriksson, 1981, 1986; Head & Bordy, 2023a, 2023b; Johnson, 1976; Stockley, 1947). This formation not only represents a significant period in Gondwana's history but also provides insights into the geological time interval between two extinction events (end-Triassic and end-Pliensbachian), capturing geological, ecological, and evolutionary events that occurred between these extinctions. Moreover, being the youngest clastic stratigraphic unit of the Karoo Supergroup, the Clarens Formation also gives insights into the final stages of basin development in the MKB, one of the largest and best-preserved foreland basin systems in southern Gondwana (Catuneanu et al., 1998).

However, despite its geological importance, the age and provenance of the Clarens Formation have been subject to limited investigations, with provenance studies only reported for a small area in the eastern MKB (Eriksson, 1981, 1986; Eriksson et al., 1994). Its Early Jurassic, specifically Pliensbachian, age determination is supported by biostratigraphy (Bordy, Abrahams, et al., 2020; Bordy & Head, 2018; du Toit, 1905; Haughton, 1924; Knoll, 2005; McPhee et al., 2017; Viglietti et al., 2020), a limited geochronological dataset from the Clarens Formation (Abrahams, 2020; Bordy, Abrahams, et al., 2020; Nxumalo, 2020; Rademan, 2018) and the radiometric dating of the continental flood basalts and associated subvolcanic complexes of the Drakensberg Group. The latter partly forms a conformable, ~2-km-thick lava pile over the Clarens Formation and partly intrudes the Karoo sedimentary units in the form of dolerites throughout southern Africa (Figure 1c; Bordy, Rampersadh, et al., 2020; Bordy et al., 2022; Duncan et al., 1997; Moulin et al., 2011; Moulin et al., 2017; Svensen et al., 2012).

Highlights

- Provenance linked to recycling of pre-existing sedimentary sequences with large-scale homogenisation of detritus.
- Early Jurassic zircon signals associated with volcanic ash plumes from the Chon Aike LIP.
- Chronostratigraphic framework established for the Clarens Formation suggests a basal Pliensbachian and younger age and un upper Toarcian and younger age.

Therefore, this study aims to utilize detrital zircon U–Pb geochronology, petrography and field sedimentology to refine the chronostratigraphic framework and provenance history for the Clarens Formation. Additionally, the study seeks to improve the understanding of the sedimentary dynamics within this aeolian system and its relationship to global Early Jurassic correlatives.

3 | GEOLOGICAL BACKGROUND

The Clarens Formation constitutes the uppermost sedimentary unit in the MKB (Figures 1 and 2), which was part of a retro-arc foreland system resulting primarily from flexural tectonics associated with subduction (Catuneanu et al., 1998). This subduction led to the development of the Pan-Gondwana Mobile Belt and its associated foreland basin system along the southern margin of Gondwana from the Late Carboniferous to the Early Jurassic (Figure 1a; Bordy et al., 2005; Catuneanu et al., 1998, 2005). During this time interval, the MKB was progressively filled with glacial, marine, fluvial, and aeolian deposits that are preserved in the Dwyka, Ecca, Beaufort and Stormberg groups of the Karoo Supergroup (Figure 1b). Representing the upper part of the Karoo Supergroup, the Upper Triassic–Lower Jurassic Stormberg Group comprises the Molteno, Elliot and Clarens formations, which collectively document a progressive aridification trend that culminated

13652117, 2024, 3, Downloaded from https://onlinelibrary.wiley.com/doi/10.1111/bre.12877 by South African Medical Research, Wiley Online Library on [14/06/2024]. See the Terms and Conditions (https://onlinelibrary.wiley.com/terms-and-conditions) on Wiley Online Library for rules of use; OA articles are governed by the applicable Creative Commons License

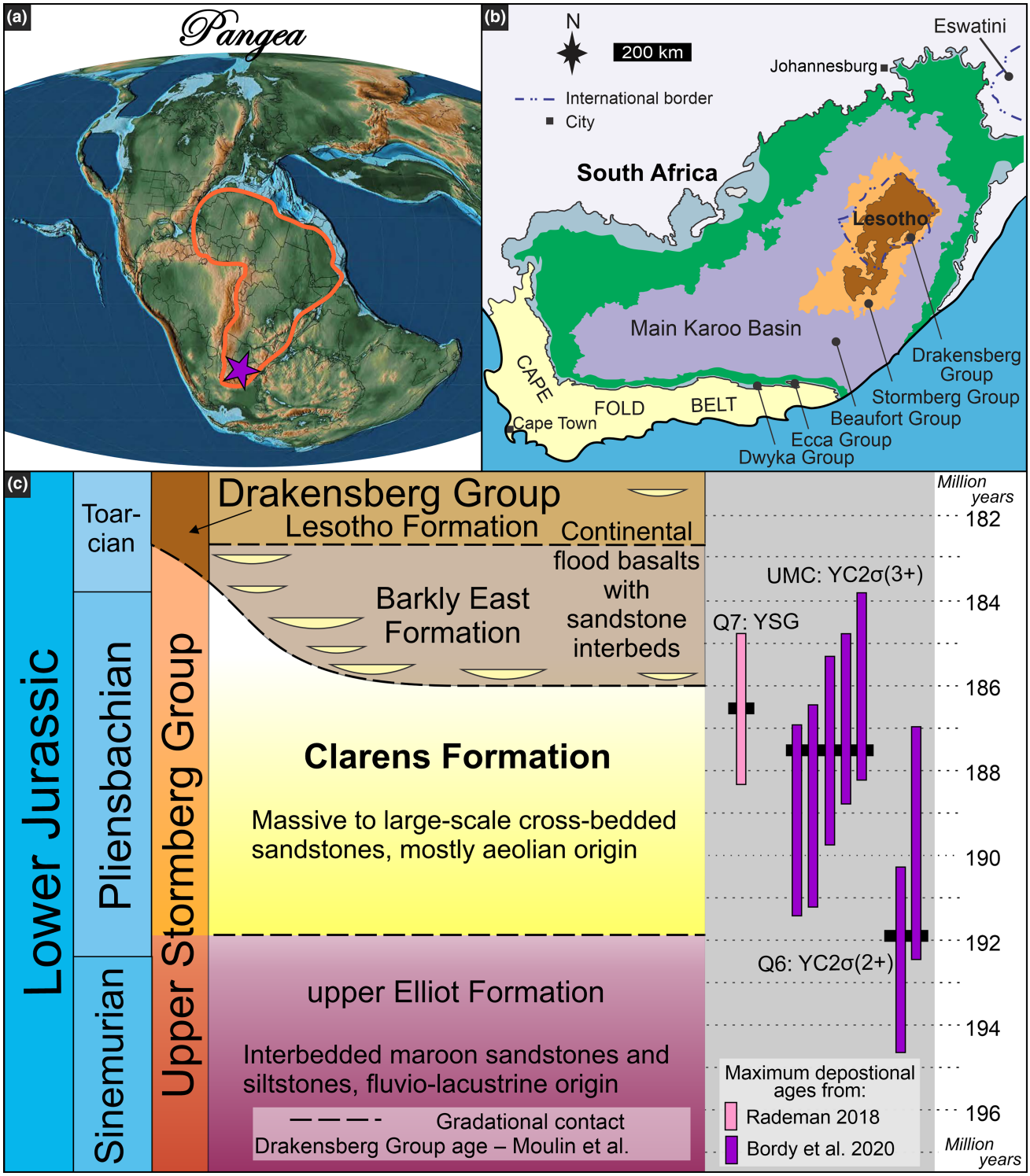


FIGURE 1 Geological context of the Clarens Formation. (a) Palaeo-geographic location of the Clarens Formation within Pangea in the Early Jurassic (base map modified after Scotese, 2014). (b) Geographical distribution of the stratigraphic groups in the Karoo Supergroup in the MKB of South Africa and Lesotho. (c) Abbreviations Q6, Q7, and UMC are sample numbers of previously published studies of the upper Karoo Supergroup, which includes the upper Stormberg (Elliot and Clarens formations) and Drakensberg groups (Bordy, Abrahams, et al., 2020; Bordy, Rampersadh, et al., 2020; Moulin et al., 2017; Rademan, 2018). YSG, youngest single grain, YC2σ(2+), youngest cluster of 2 or more zircon dates that overlap at 2SE.

in the deposition of the aeolianite-dominated Clarens Formation (Figure 1c; Bordy et al., 2005, 2021; Bordy, Abrahams, et al., 2020).

Overlying and pervasively intruding the upper Karoo sedimentary sequence are the continental flood basalts and their subvolcanic counterparts of the Drakensberg

13652117, 2024, 3, Downloaded from https://onlinelibrary.wiley.com/doi/10.1111/bre.12877 by South African Medical Research, Wiley Online Library on [14/06/2024]. See the Terms and Conditions (https://onlinelibrary.wiley.com/terms-and-conditions) on Wiley Online Library for rules of use; OA articles are governed by the applicable Creative Commons License

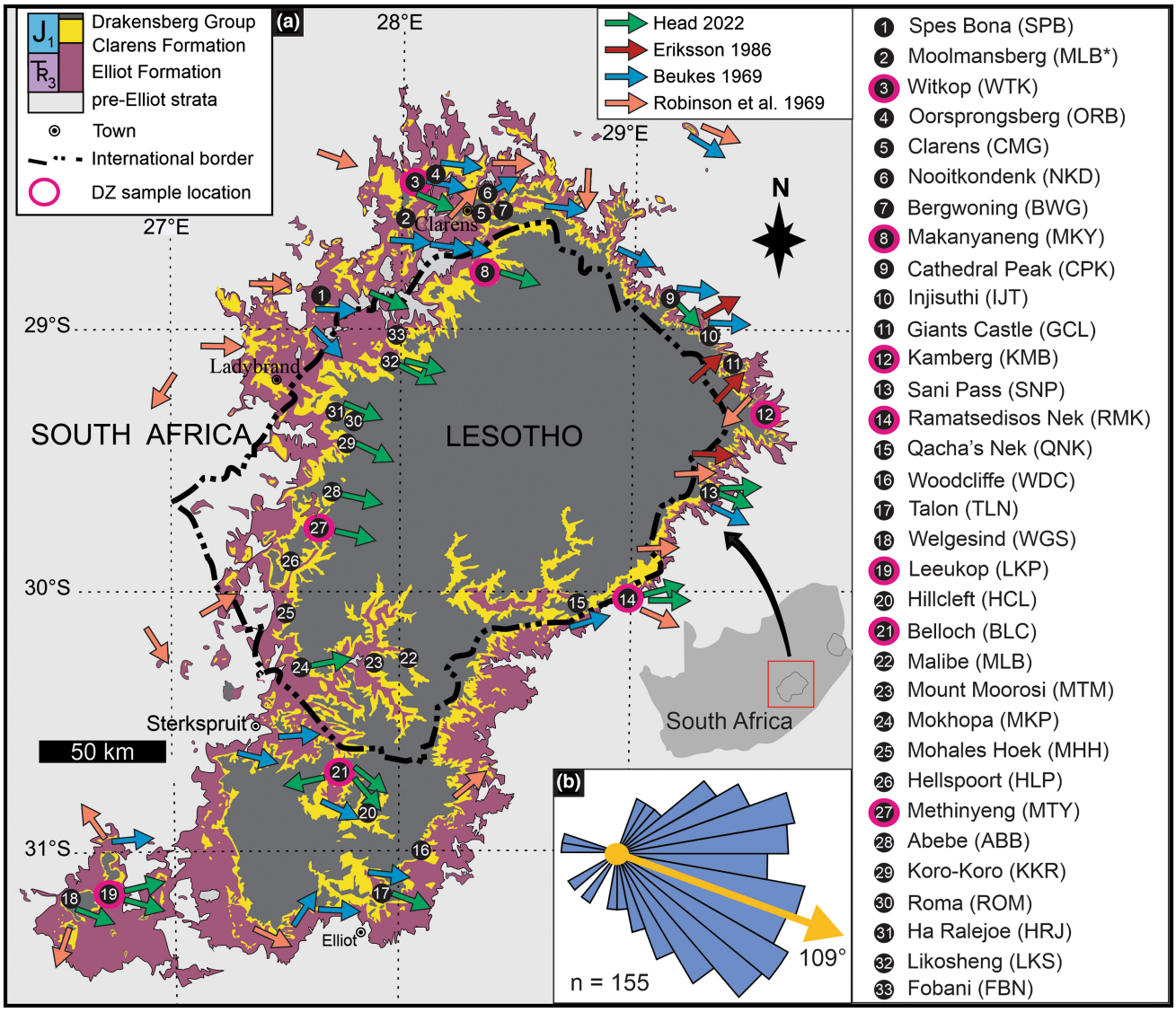


FIGURE 2 Spatial distribution of palaeo-current data and rock samples from the Clarens Formation. (a) Geological map of the upper Karoo Supergroup with sample locations of this study shown in numbered circles. DZ/magenta circles—samples used for detrital zircon U–Pb dating; coloured arrows – subregional palaeo-current directions from various studies. (b) Summary rose diagram for the Clarens Formation in the MKB from palaeo-current measurement of this study. *n*—total number of measurements; yellow arrow—the main palaeo-current vector.

Group, associated with igneous activities in the Karoo-Ferrar Large Igneous Province (Figure 1b,c; Duncan et al., 1997; Moulin et al., 2017; Svensen et al., 2006). During the final stages of the MKB history, during the Pliensbachian–early Toarcian, sedimentary and igneous activities co-existed in an increasingly extensional tectonic setting that ultimately led to the disintegration of Gondwana (Bordy, Rampersadh, et al., 2020; Bordy et al., 2021, 2022; Moulin et al., 2017; Muir et al., 2020). In post-Karoo times, the fill of the MBK was extensively eroded. Nevertheless, the present-day distribution of the upper Karoo (Figures 1b and 2a) is interpreted to represent the northern extent of the 'Stormberg Basin', the generation of which is linked to the first-order orogenic unloading of the foreland system in the Early Jurassic (Bordy et al., 2004, 2005; Catuneanu et al., 1998; Hanson et al., 2009). This orogenic unloading also facilitated the reworking of pre-existing Karoo sediments into the 'Stormberg Basin' (i.e., the foresag itself).

In addition to the MKB, the aeolian Clarens Formation is exposed in several contemporaneous basins within South Africa, such as the Springbok Flats, Lebombo, Tshipise, Tuli and Lephalale-Ellisras basins (Bordy & Catuneanu, 2002; Bordy & Head, 2018; Smith et al., 1993). Moreover, coeval aeolianites are also found in Namibia (Etjo Formation), Zimbabwe (Forest Sandstone) and Botswana (Ntane, Tsheung and Bodibeng Sandstone formations; Bordy & Head, 2018; Holzförster et al., 1999;

13652117, 2024, 3, Downloaded from https://onlinelibrary.wiley.com/doi/10.1111/bre.12877 by South African Medical Research, Wiley Online Library on [14/06/2024]. See the Terms and Conditions (https://onlinelibrary.wiley.com/terms-and-conditions) on Wiley Online Library for rules of use; OA articles are governed by the applicable Creative Commons License

Stagman, 1978; Thompson, 1975; Visser, 1984; Smith et al., 1993), highlighting the extensive palaeo-geographic distribution of this Early Jurassic erg system within southwestern Gondwana (Figure 1a). The conformable lower contact of the Clarens Formation with the underlying Elliot Formation (Figure 1c) is considered transitional and is marked by interbedded red beds and cream to pale-coloured aeolian sandstones in the basal zone. The conformable upper contact with the Drakensberg Group is sharp due to the lithological contrast between the sedimentary and igneous rocks. Nonetheless, this complex interbedded relationship is also transitional and indicates that aeolian and volcanic processes coexisted in the Early Jurassic (Figure 1c; Bordy, Rampersadh, et al., 2020; Bordy et al., 2021, 2022; Moulin et al., 2017).

The Clarens Formation in the MKB is dominated by massive to large-scale cross-bedded, fine- to very fine-grained silty sandstone, having a cream, pink to pale green colour. The massive units have been interpreted to reflect a continuum of erg marginal deposits from migrating dunes to sand sheets and loess (Head & Bordy, 2023b), whereas large-scale cross-bedded sandstones reflect migrating dunes (Beukes, 1969, 1970; Bordy & Head, 2018; Eriksson, 1981, 1986; Head & Bordy, 2023a, 2023b). Lenticular sandstones with ripple marks, ripple cross-lamination, desiccation cracks and horizontal lamination are mostly confined to the lower and upper parts of the formation (Beukes, 1969, 1970; Bordy & Head, 2018; Eriksson, 1981, 1986; Head & Bordy, 2023a; Johnson, 1976; Van Dijk & Eriksson, 2021). Mudstones are comparatively rare and generally appear as thin (<30 cm), lenticular beds that are interbedded with sandstones. The thickness of the Clarens Formation varies across the MKB, ranging from 10 to over 300 m. However, a typical thickness of 100–150 m provides a reasonable representation of the unit's regional thickness (Beukes, 1969; du Toit, 1905, 1918; Eriksson, 1981, 1986; Head, 2022; Johnson, 1976).

Petrographic analysis of the Clarens Formation reveals a dominant composition of quartz-rich feldspathic wackes, with subordinate arkosic arenites or subarkosic to quartz wackes (Beukes, 1970; Bordy & Head, 2018; Eriksson, 1986; Eriksson et al., 1994). The dominant silty sandstones show a medium to very fine-grained texture and generally moderate to poor sorting. Comparatively, the sand grains are more rounded than the silt grains. The heavy mineral suite consists of zircon, rutile, tourmaline, epidote, titanite, garnet, riebeckite and hornblende (Beukes, 1970; Eriksson et al., 1994; Koen, 1955). As mentioned, only a limited dataset of maximum depositional ages (MDA) based on U–Pb detrital zircon data is available for the Clarens Formation (Figure 1c; Abrahams, 2020; Bordy, Abrahams, et al., 2020; Bordy, Rampersadh, et al., 2020; Nxumalo, 2020; Rademan, 2018). The existing MDA are shown in Figure 1, where sample Q6 has an MDA of 191.1 ± 1.5 (Bordy, Abrahams, et al., 2020; Bordy, Rampersadh, et al., 2020), sample UMC has an MDA of 185.7 ± 1.2 (Bordy, Abrahams, et al., 2020a) and sample Q7 has an MDA of 186.7 ± 1.6 (Rademan, 2018).

The diverse fossil assemblage of the Clarens Formation includes vertebrates (tetrapod bone fossils, fossil fish), invertebrates (crustaceans, insects), various ichnofossils of both vertebrates and invertebrates, plant impressions and petrified wood (see references in Bordy & Head, 2018; Abrahams et al., 2021; Bordy et al., 2021). It is therefore envisaged that the Clarens Formation hosted locally diverse palaeo-ecosystems throughout its deposition, which continued well beyond the initiation of the large-scale continental flood basalts in the earliest Toarcian (Bordy et al., 2021, 2022; Duncan et al., 1997; Moulin et al., 2011, 2017; Muir et al., 2020; Svensen et al., 2012). This interplay between the aeolian system and ongoing volcanism is suggested to have started during a proposed early onset of the Karoo volcanism between 187 and 185 Ma (Bordy et al., 2021; Moulin et al., 2017).

Palaeo-current measurements from the large-scale, cross-bedded sandstones indicate that a prominent west-to-east wind regime existed over southwestern Gondwana during the Early Jurassic (Figure 2; Beukes, 1969, 1970; Bordy, 2008; Bordy et al., 2009; Bordy & Head, 2018; du Toit, 1905; Eriksson, 1981; Eriksson, 1986). Overall, the dominance of both large-scale, cross-bedded and massive sandstones, especially in the middle part of the formation, point to the development of aeolian conditions with migrating dunes and windblown dust (Head & Bordy, 2023b). The lenticular sandstones and mudstones, confined to the lower and upper part of the formation, are suggestive of wet conditions within the erg system (Beukes, 1969, 1970; Bordy, 2008; Bordy & Head, 2018; Head & Bordy, 2023a). These features, concentrated in three stratigraphic zones, prompted Beukes (1969, 1970) to explain them with wet-dry-wet climatic megacycles during the deposition of the formation. In contrast to this notion of temporal climatic changes, Eriksson (1981, 1986) defined spatial domains in the Clarens Formation and suggested the co-existence of a dry inner erg to the west of the basin and a wet desert setting in the south, southeast, and east of the basin.

4 | METHODS

To investigate the provenance of the Clarens Formation, a total of 110 rock samples were collected for petrographic analysis across the basin (Figure 2). Petrographic analysis was carried out using a transmitted light microscope

13652117, 2024, 3, Downloaded from https://onlinelibrary.wiley.com/doi/10.1111/bre.12877 by South African Medical Research, Wiley Online Library on [14/06/2024]. See the Terms and Conditions (https://onlinelibrary.wiley.com/terms-and-conditions) on Wiley Online Library for rules of use; OA articles are governed by the applicable Creative Commons License

and employing the Gazzi-Dickinson point-counting technique, where a total of 300 points was counted per sample for a representative estimate of the modal compositions (Gazzi, 1966; Ingersoll et al., 1984). Heavy minerals were not included in the point counting tables but rather evaluated as a separate step to identify their spatial and stratigraphic distribution throughout the basin. The point-counting results are illustrated

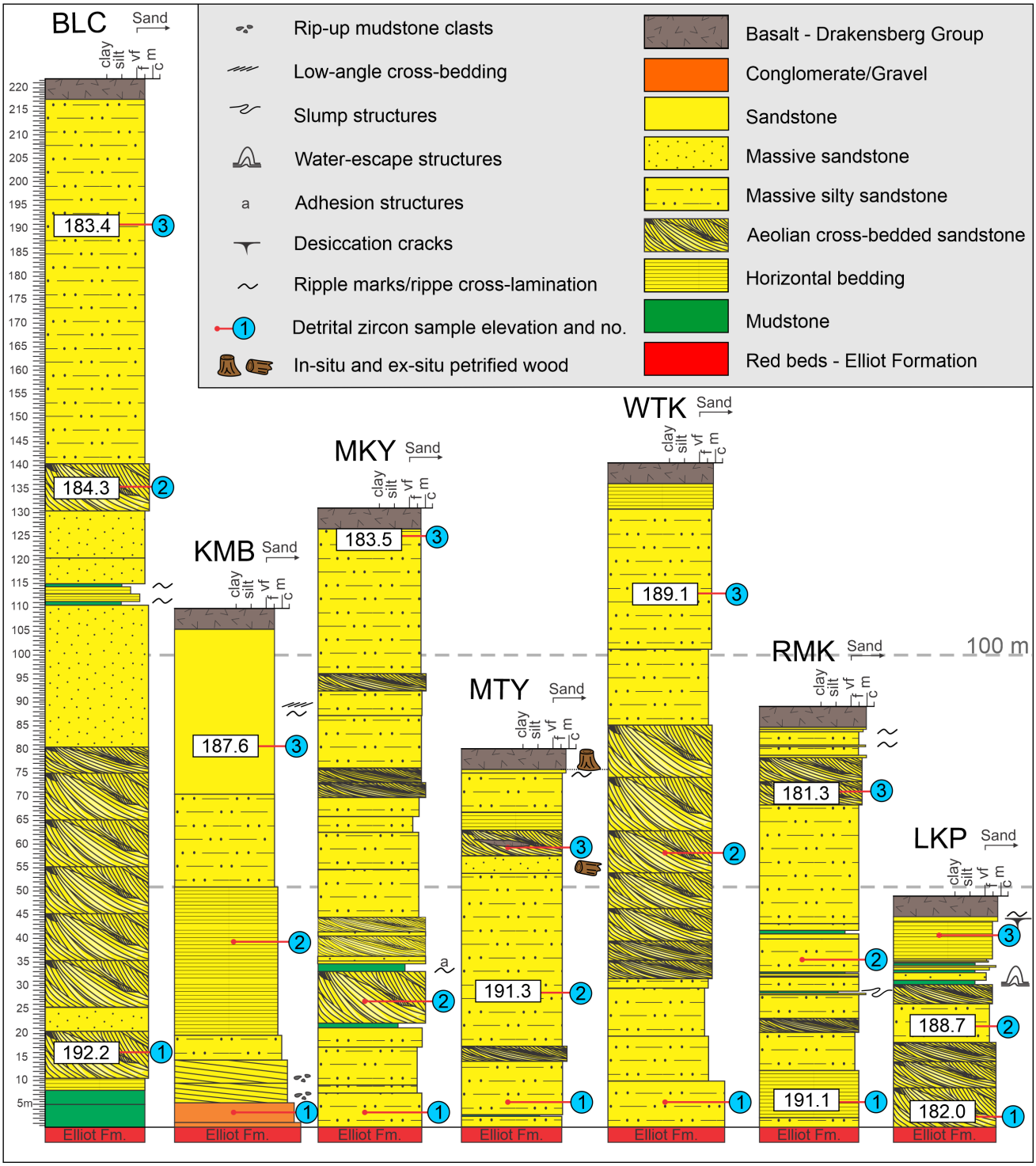


FIGURE 3 Sedimentary logs from this study with stratigraphic locations of detrital zircon samples and preferred MDAs in the Clarens Formation as detailed in Table 1. Note that the overlying 3-letter code refers to the location name, while samples labelled '1', '2' and '3' are from the three different stratigraphic intervals ('zones') of the Clarens Formation, and when combined, give the various sample names—e.g., BLC-01. See Figure 2 for log abbreviations and locations within the study area. For associated 2 SE uncertainty, see Table 1.

13652117, 2024, 3, Downloaded from https://onlinelibrary.wiley.com/doi/10.1111/bre.12877 by South African Medical Research, Wiley Online Library on [14/06/2024]. See the Terms and Conditions (https://onlinelibrary.wiley.com/terms-and-conditions) on Wiley Online Library for rules of use; OA articles are governed by the applicable Creative Commons License

following the ternary sandstone classification schemes of Krynine (1948), Crook (1960), Folk (1980) and Dickinson (1985) and updated by Garzanti, Dinis, et al. (2018) and Garzanti (2019) to remove subjectivity related to ambiguous historical terminology. Sandstone point counting data are available as Appendix S1.

In addition, 21 rock samples (Figure 3) were collected for U–Pb dating using laser ablation inductively coupled plasma ionization mass spectrometry (LA-ICP-MS) to improve the chronostratigraphy of the Clarens Formation. Samples for U–Pb zircon dating were collected from each of the stratigraphic intervals ('zones') as defined by Beukes (1969, 1970) to ensure a complete spatiotemporal representation of the Clarens Formation (Figure 2a). The samples were prepared at the Central Analytical Facilities (CAF) at Stellenbosch University in South Africa. Frantz magnetic and heavy liquid (tetrabromoethane) mineral separation was preceded by crushing, milling, and panning of the samples. Zircons were hand-picked and mounted in 25 mm epoxy resin discs and polished to expose the interior of the mineral grains. The zircons were then imaged at the CAF using a Scanning Electron Microscope (SEM Zeiss Merlin) equipped with a CL detector to allow a zircon micro-textural analysis (Corfu et al., 2003) prior to LA U–Pb dating. One hundred to a hundred and twenty (100–120) spots were selected at random and ablation spots for the U–Pb dating were guided by intra-crystal zoning based on CL-imagery and zircon micro-textural analysis, with different growth zones targeted as appropriate in order to capture distinct zircon growth events. To evaluate zircon morphology, the long axis, short axis and roundness of zircons were measured using Image-J software to calculate the elongation factor (Gärtner et al., 2013).

Laser Ablation-ICP-MS U–Pb analysis was completed at the mass spectrometry facility in the School of Geosciences, University of the Witwatersrand (Johannesburg, South Africa). A detailed method description including analysis parameters and the zircon U–Pb data tables, can be found in Appendices S2–S6. Data reduction was conducted using Iolite v 3.5 (Paton et al., 2011) utilizing VizualAge (Petrus & Kamber, 2012), including the calculation of absolute ages and uncertainties (2 SE). Concordia (Wetherill plots—supplementary material), cumulative percentage plots and kernel density estimates (KDE) were prepared using IsoplotR (Vermeesch, 2018); a 97%–103% concordance threshold was applied to the age results before plotting the data as KDE diagrams. In addition, for zircon ages <1 Ga the $^{206}Pb/^{238}U$ date was used, while for zircon ages >1G the $^{207}Pb/^{206}U$ date was used for the KDE plot. Concordance was calculated using both the $^{206}Pb/^{238}U$ versus $^{207}Pb/^{206}Pb$ and $^{206}Pb/^{238}U$ versus $^{207}Pb/^{235}U$ ratios, where a $^{206}Pb/^{238}U$ versus $^{207}Pb/^{235}U$ ratio applied to dates younger than 1 Ga and a $^{206}Pb/^{238}U$ versus $^{207}Pb/^{206}Pb$ ratio was applied to dates older than 1 Ga.

5 | RESULTS

5.1 | Petrography

The sandstones and sandy siltstones are moderately to well sorted, and some samples show poor sorting. Compared to samples from the massive sandstone deposits, a slightly better sorting characterizes the large-scale, cross-bedded sandstones. The sandstones are composed of medium- to very fine-grained sand to sandy silt. Most grains are elongated, sub-angular to sub-rounded and the larger grains are generally better rounded (Figure 4). The grains are well packed with long and point contacts. In most samples, the matrix (here defined as grains <30 μm in diameter—Gazzi, 1966; Garzanti, 2016) represents 5%–10% of the rock (i.e., framework grains represent 90%–95%). Regional trends in grain shape and size in the Clarens Formation are detailed in Head (2022) and Head and Bordy (2023b). However, it should be noted that except for a slight west-to-east fining (Beukes, 1969), no spatiotemporal grain morphology and size trends were detected in our studies.

Petrographic analysis indicates that the Clarens Formation sandstones are composed of quartzose sandstones with a mean composition of 74% quartz, 22% feldspar and 4% rock fragments (i.e., mean $Q_{74}F_{22}L_4$). Five out of the 110 samples are either pure quartzose (CMG-02; KKR-02; MTM-01) or quartz-rich feldspatho-quartzose (CPK-04; BWG-04) sandstones. The detailed sandstone classification of each sample can be found in Appendix S1. Monocrystalline quartz dominates (96%) over polycrystalline quartz, where monocrystalline quartz shows both non-undulatory (60%) and undulatory extinction under cross-polarized light. Polycrystalline quartz grains contain mostly less than four crystals with non-sutured boundaries. The feldspar component is mostly plagioclase (95%) that is characterized by albite twinning with minor K-feldspar in the form of perthite (Figure 4). Untwined feldspar was distinguished from quartz by incipient alteration causing a cloudier appearance. Lithic fragments are extremely rare, with grains of chert and shale representing between 1% and 3% of the counted modal grains. There is a slightly higher lithic content in the southern, northern and eastern outcrop areas, as compared to that of the western outcrop area (Figure 5).

Heavy minerals identified from petrographic analysis in the samples are zircon, tourmaline, rutile, green to brown

13652117, 2024, 3, Downloaded from https://onlinelibrary.wiley.com/doi/10.1111/bre.12877 by South African Medical Research, Wiley Online Library on [14/06/2024]. See the Terms and Conditions (https://onlinelibrary.wiley.com/terms-and-conditions) on Wiley Online Library for rules of use; OA articles are governed by the applicable Creative Commons License

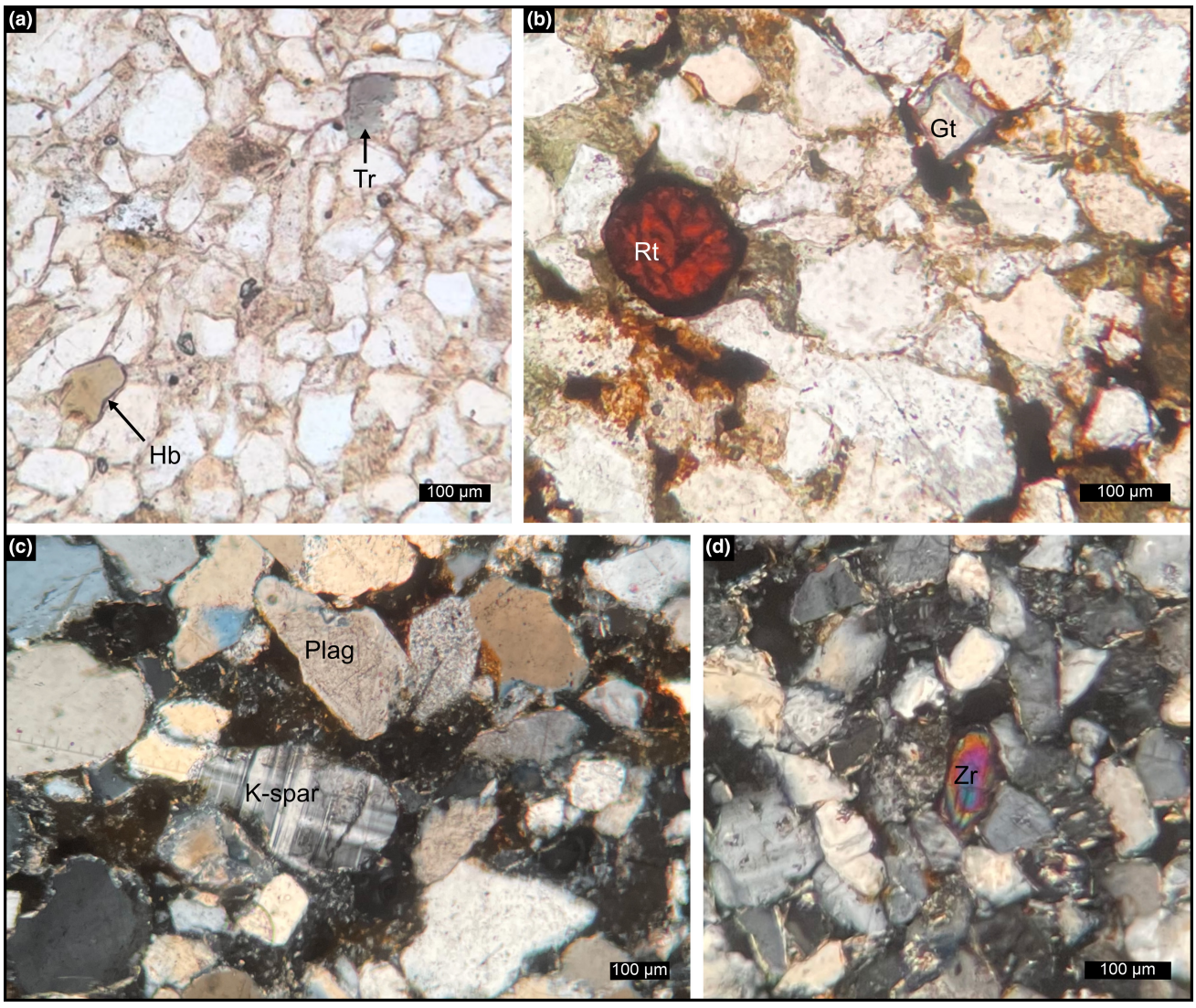


FIGURE 4 Photomicrographs of common and accessory minerals in the Clarens Formation. (a) Yellow-brown hornblende (Hb) and tourmaline (Tr) in a quartz-dominated sandstone—PPL. (b) Rutile (Rt) and garnet (Gt) amongst quartz grains in PPL. (c) K-feldspar (K-Spar) and plagioclase (Plag) amongst quartz grains in XPL. (d) Zircon (Zr) amongst grains in XPL. Note that the moderately to well-sorted sand grains are subrounded to subangular.

hornblende, garnet, epidote, titanite and opaque minerals (Figure 4). The most abundant accessory minerals are zircon, tourmaline and rutile (ZTR), which commonly occur together. These minerals are stable and capable of surviving several cycles of sedimentary reworking. Spatial or temporal trends were not observed in the distribution of heavy minerals across the outcrop area. Garnets lack alteration features, while other unstable minerals, such as hornblende and epidote, exhibit initial corrosion textures (Figure 4a,b). Samples from the lowermost Clarens Formation at Kamberg (KMB) were collected from rocks interpreted as channel deposits of ephemeral stream origin (Head, 2022). These samples (KMB-01, KMB-02) display a larger grain size (grit to very coarse-grained sand) and contain abundant polycrystalline quartz consisting of sutured crystals (Figure 6a,b,d). Lithic fragments of volcanic origin (Lv: basalt fragments) were identified in samples interpreted as debris flow deposits in the uppermost Clarens Formation at Talon (TLN; Figure 6c; see Head, 2022).

5.2 | Palaeo-currents

In this study, the palaeo-flow directions measured from 155 large-scale, cross-bedded sandstones, mostly from the middle zone of the formation, indicate a strong west-to-east wind regime with a mean vector of 109° (±35.75°, 1 SD) and a consistency ratio of 0.81 (Figure 2b). Despite this strong west-to-east trend, localized variations in palaeo-currents are observed to such an extreme that, for example, at Balloch, foresets dip towards the west (Figure 2a).

13652117, 2024, 3, Downloaded from https://onlinelibrary.wiley.com/doi/10.1111/bre.12877 by South African Medical Research, Wiley Online Library on [14/06/2024]. See the Terms and Conditions (https://onlinelibrary.wiley.com/terms-and-conditions) on Wiley Online Library for rules of use; OA articles are governed by the applicable Creative Commons License

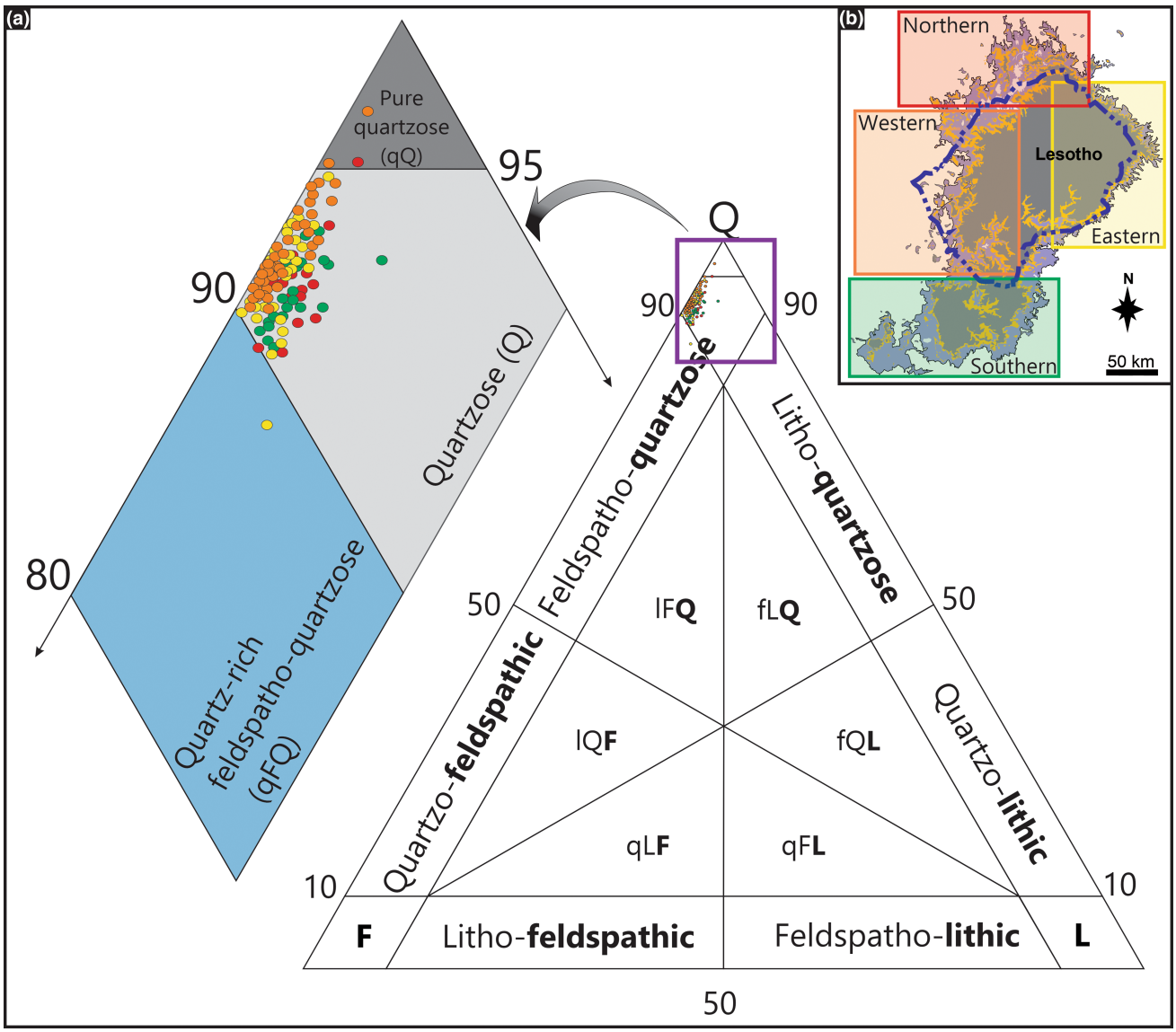


FIGURE 5 Sandstone composition of Clarens Formation samples (using the classification of Garzanti, 2019) (a). For regional sample locations, see colour coded map inset in (b). F, K-feldspar and plagioclase; L, Lithic fragments including chert; Q, total quartz. Note that the samples taken from the northern (red), eastern (yellow) and southern (green) sampling areas contain relatively more lithics than the western (orange) samples.

5.3 | Detrital zircon U–Pb geochronology

5.3.1 | Provenance

A total of 21 samples were analysed, where 2341 ablated spots resulted in 1702 concordant zircon age dates. Overall, the zircon data from the Clarens Formation shows a spread of U–Pb dates from ca. 3300 to 181 Ma, with most samples showing a broadly similar distribution of dates in slightly different proportions. Zircon data was plotted as KDE plots (Figures 7 and 8) to visualize the data by a continuous probability density curve. The samples are dominated by a Cambrian to early Neoproterozoic component (Pan-African: 490–650 Ma) that represents roughly 30%–50% of each sample, followed by Tonian-Stenian (Grenvillian: 0.9–1.1 Ga) age fractions that represent 5%–20% of each sample. Permian age fractions (298.9–251.9 Ma) represent between 5% and 21%, whereas Ordovician age fractions (458.4–443.8 Ma) account for 2%–20% of each sample. Middle Palaeoproterozoic (2.5–1.6 Ga) and Archean (>2.5 Ga) age fractions are rare (Figures 7 and 8). The youngest population identified in the zircon samples have an Early Jurassic age that varies from 192 to 181 Ma (Sinemurian to Toarcian) and is very scarce compared to other age fractions.

Sample KMB-01 shows a notable divergence from the overall zircon date distribution and is associated with ephemeral channel deposits from zone 1, as described

13652117, 2024, 3, Downloaded from https://onlinelibrary.wiley.com/doi/10.1111/bre.12877 by South African Medical Research, Wiley Online Library on [14/06/2024]. See the Terms and Conditions (https://onlinelibrary.wiley.com/terms-and-conditions) on Wiley Online Library for rules of use; OA articles are governed by the applicable Creative Commons License

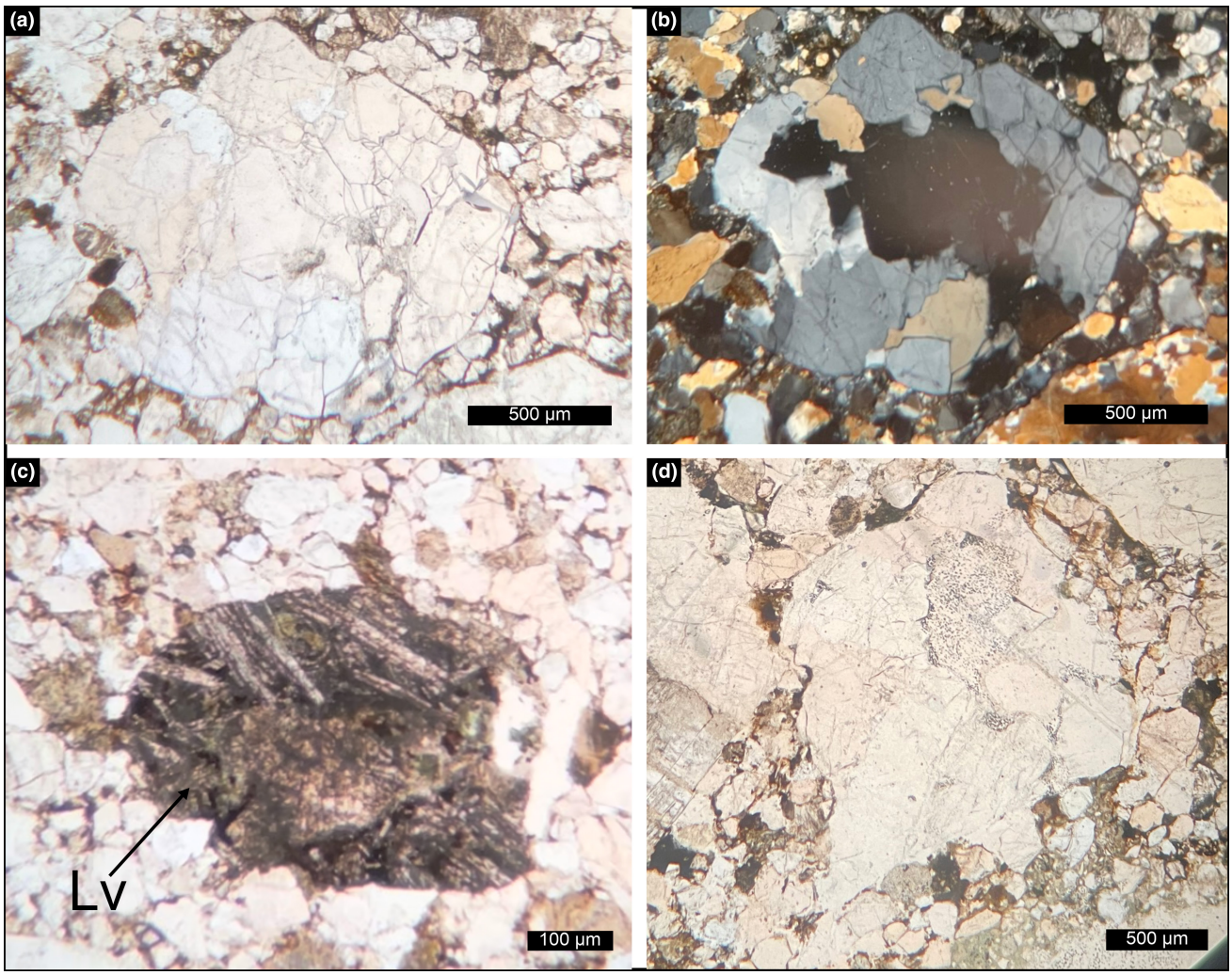


FIGURE 6 Photomicrographs of rare lithic fragments in the Clarens Formation. (a, b) Polycrystalline quartz in PPL (a) and XPL (b). (c) Volcanic lithic fragment (Lv: basalt grain) with jagged outline in the uppermost part of the Clarens Formation at Talon—PPL. (d) Polycrystalline quartz in the lowermost Clarens Formation at Kamberg. See Figure 2 for sample locations.

by Head (2022). In this sample, a Tonian-Stenian (1000 to 720 Ma) age fraction is dominant, while the Permian age fraction is significantly reduced (Figures 7 and 8). Furthermore, this dominant age fraction is not observed in the overlying samples from the Clarens Formation in this area (zones 2 and 3). For the up-stratigraphy samples above KMB-01, a Cambrian to Early Neoproterozoic (Pan-African) age fraction becomes dominant, as observed in other sample locations.

Sample BLC-01 shows a prominent Cambrian to Early Neoproterozoic (Pan-African) component, which is also the largest Pan-African component from all samples, whereas its Tonian-Stenian (Grenvillian) component is markedly smaller when compared to the overall age fraction trends. The highest Permian age fraction is observed at Witkop in the zone 3 sample (WTK-03), while a general trend for samples collected from the northern part of the basin indicates an up-stratigraphy increase in Permian age fractions (WTP and KMB). Grain elongation and roundness measurements did not reveal any trends in zircon shape that could be correlated with age. While grain elongation and roundness lack a consistent trend, the Early Jurassic zircon grains are euhedral to subhedral and show oscillatory zoning typical in zircons of igneous origin (Figure 9).

5.3.2 | MDA determinations

Maximum depositional ages (Table 1, Figures 7, 8, 10 and 11) were derived using metrics discussed by, or modified from, Dickinson and Gehrels (2009) and Coutts et al. (2019). These include: (1) youngest single grain [YSG] and (2) an additional method similar to Dickinson and Gehrels (2009) and Coutts et al. (2019), where the youngest cluster of 2 or more zircons overlap at 2σ [YC2 σ(2+)]

13652117, 2024, 3, Downloaded from https://onlinelibrary.wiley.com/doi/10.1111/bre.12877 by South African Medical Research, Wiley Online Library on [14/06/2024]. See the Terms and Conditions (https://onlinelibrary.wiley.com/terms-and-conditions) on Wiley Online Library for rules of use; OA articles are governed by the applicable Creative Commons License

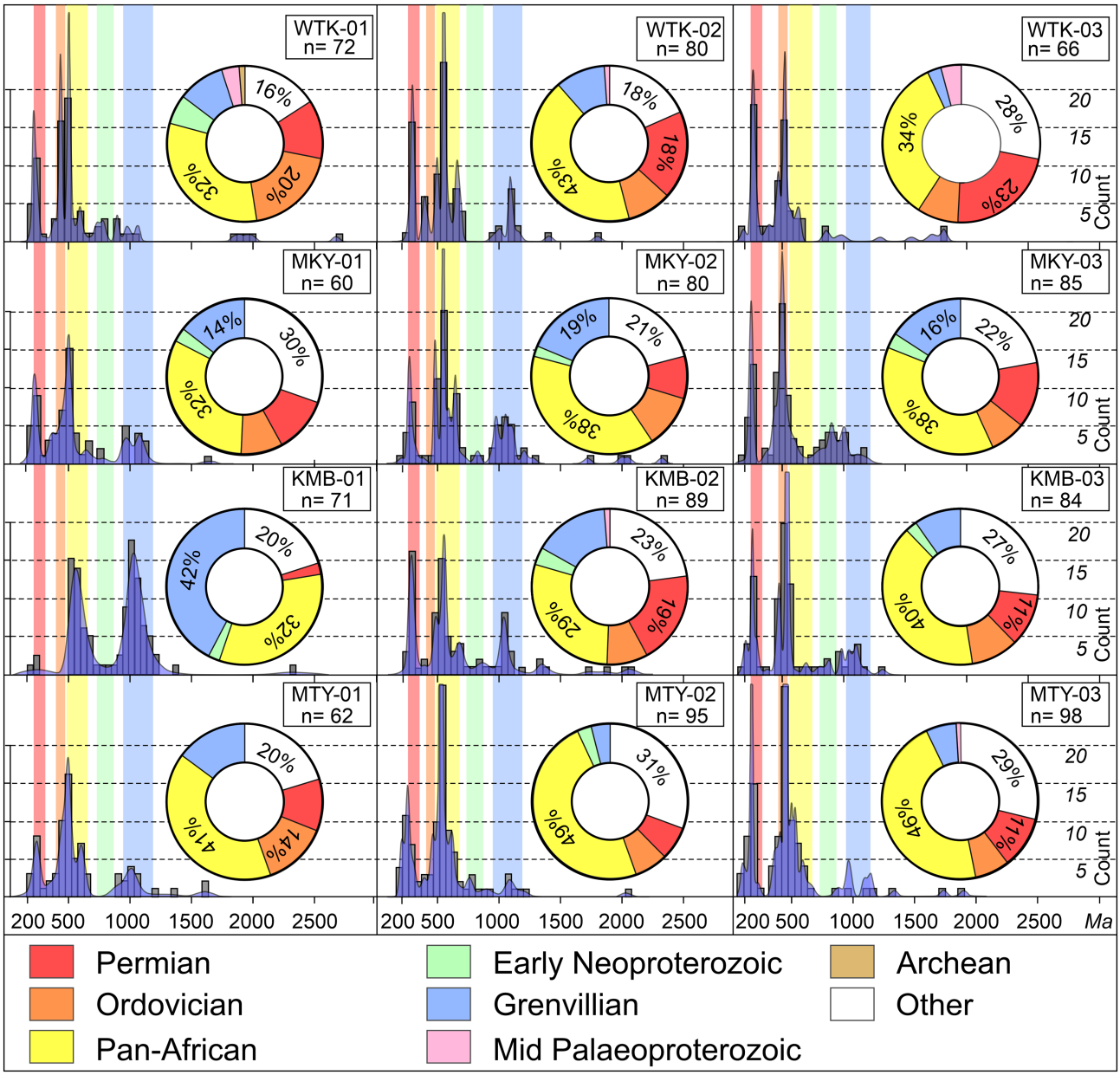


FIGURE 7 Kernel density estimates (KDE) of 12 samples from the northern half of the outcrop area combined with donut plots depicting the percentage of each age fraction that can be attributed to the large-scale tectonic events listed in the legend. The white boxes show the sample label and the number of concordant dates plotted in each diagram. See Figure 2 for sample locations and Figure 3 for the relative stratigraphic position of the samples within each sampled section (1: bottom, 2: middle, 3: top).

(Bordy, Abrahams, et al., 2020). Clustered MDA calculations were made in IsoplotR using the weighted mean function.

According to Coutts et al. (2019), single grain methods, such as youngest single grain (YSG), youngest detrital zircon (YDZ) and weighted average of the youngest grains (Y3Z) are all prone to producing calculated MDA results that are younger than the true depositional age (TDA) when obtained from large n-datasets or sample populations with abundant near-depositional age zircon crystals. This may be caused by cryptic or undetected Pb loss and field and lab contamination (Coutts et al., 2019, Herriott et al., 2019; Kortyna et al., 2023). However, Sharman and Malkowski (2020) noted that MDA calculations based on datasets with limited sampling of near-depositional age zircon grains, attributed to their scarcity, may yield results that closely approximate the TDA.

Alternatively, youngest grain cluster techniques are more likely to produce MDA results that can fit into existing chronostratigraphic constraints since these are less prone to be influenced by single zircon dates that are too young (Coutts et al., 2019; Kortyna et al., 2023; Sharman &

13652117, 2024, 3, Downloaded from https://onlinelibrary.wiley.com/doi/10.1111/bre.12877 by South African Medical Research, Wiley Online Library on [14/06/2024]. See the Terms and Conditions (https://onlinelibrary.wiley.com/terms-and-conditions) on Wiley Online Library for rules of use; OA articles are governed by the applicable Creative Commons License

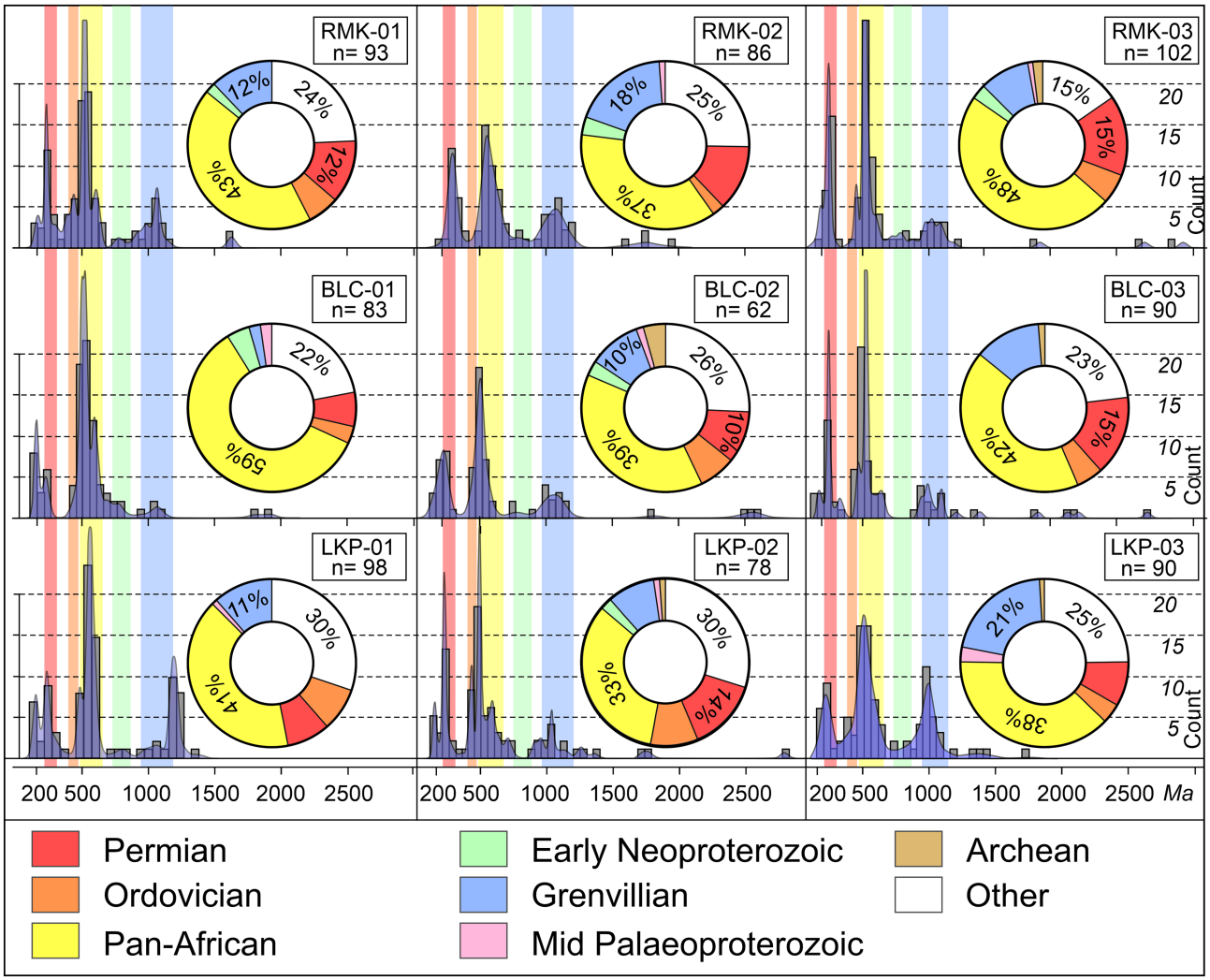


FIGURE 8 Kernel density estimates (KDEs) of nine samples from the southern half of the outcrop area combined with donut plots depicting the percentage of each age fraction that can be attributed to the large-scale tectonic events during time periods listed in the legend. The white boxes show the sample label and the number of concordant dates plotted in each diagram. See Figure 2 for sample locations and Figure 3 for the relative stratigraphic position of the samples within each sampled section (01: bottom, 02: middle, 03: top).

Malkowski, 2020), although these calculations have also been shown to produce MDAs that are younger or older than the TDA (Schwartz et al., 2023).

Given some of these limitations, an approach similar to that adopted by Bordy, Abrahams, et al. (2020) and Bordy, Rampersadh, et al. (2020) was taken to select the appropriate MDA metric. In this approach, a preferred MDA may reflect any of the metrics that can be justified as meaningful in terms of the broader geological evidence, including existing biostratigraphic and geochronological constraints that are chrono-stratigraphically significant. For metrics where an MDA calculation was deemed meaningless or chrono-stratigraphically inconsistent (outside of the existing constraints), no preferred metric was selected. In this study, chrono-stratigraphically insignificant MDA results represent MDAs that were older than the currently accepted age of the Clarens Formation as determined by a limited number of published detrital zircon data (Bordy, Abrahams, et al., 2020), the biostratigraphy of the Clarens Formation (Knoll, 2005; Viglietti et al., 2020), and most significantly, the radiometric age determinations of the conformably overlying Drakensberg Group (Duncan et al., 1997; Moulin et al., 2011, 2017; Svensen et al., 2012), supported by robust magnetostratigraphic, chemostratigraphic and petrological investigations (e.g., Duncan et al., 1997; Jay et al., 2018; Marsh et al., 1997). Chrono-stratigraphically non-significant MDA results may be attributed to a lack of zircons with near-depositional ages coupled with the oversampling of recycled zircons or undetected Pb loss (Andersen, Kristoffersen, et al., 2016; Andersen, Elburg, et al., 2016; Bordy et al., 2020a; Sharman & Malkowski, 2020).

Overall, 11 of the 21 samples from this study yielded Early Jurassic MDAs that are relevant within the

13652117, 2024, 3, Downloaded from https://onlinelibrary.wiley.com/doi/10.1111/bre.12877 by South African Medical Research, Wiley Online Library on [14/06/2024]. See the Terms and Conditions (https://onlinelibrary.wiley.com/terms-and-conditions) on Wiley Online Library for rules of use; OA articles are governed by the applicable Creative Commons License

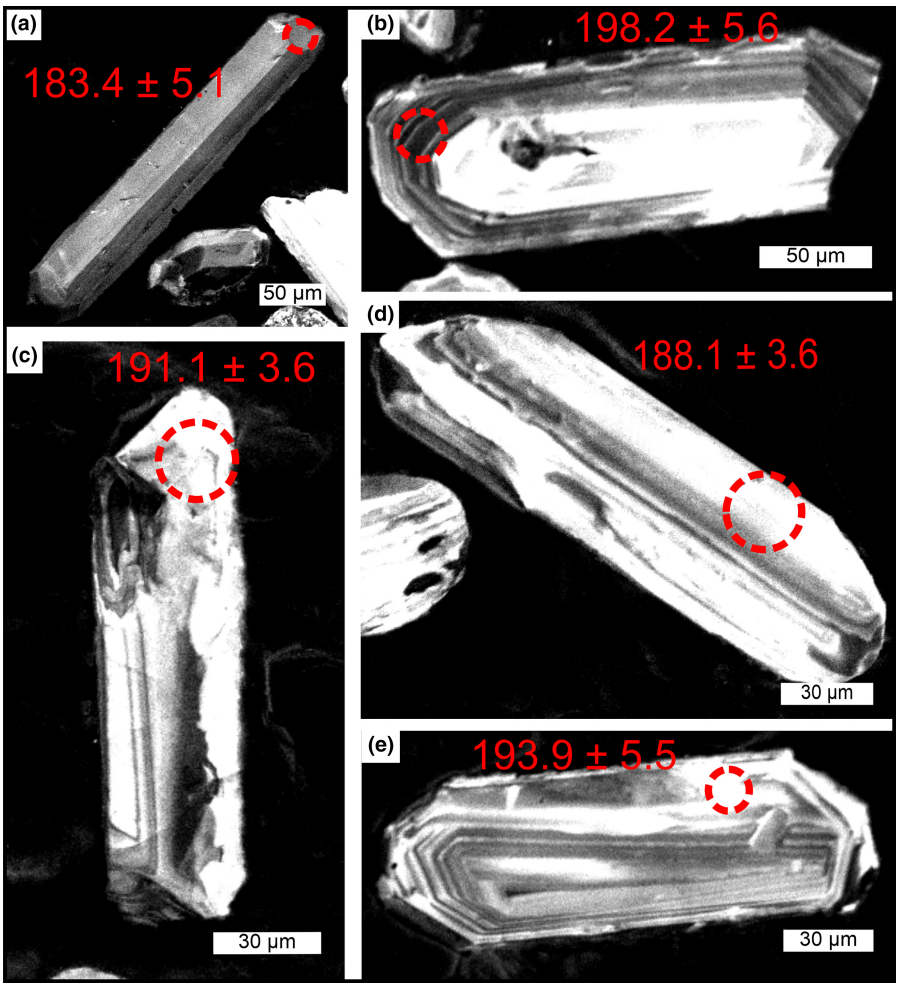


FIGURE 9 CL images of zircons with youngest dates of samples BLC-02-28, BLC-01-96, RMK-01-32, RMK-02-85 and BLC-01-38, respectively. (a–e) Zircons with oscillatory zoning typical of igneous origin, with euhedral to subhedral shape. Red circles represent ablation spots; $^{206}Pb/^{238}U$ concordant dates (Ma) ±2 SE uncertainty. Error propagation using iolite involves combining excess uncertainty (from "pseudosecondary standards") with internal errors for each analysis (Paton et al., 2010).

context of the existing biostratigraphic and geochronological age estimates (Table 1—preferred MDAs). These Early Jurassic zircon age fractions represent a small portion (roughly 2.5%) of the overall zircon population and appear throughout the rock succession of the Clarens Formation (Figure 11). The preferred MDAs cluster around two age ranges throughout the Clarens Formation. Firstly, samples from the lower to middle zones show a noteworthy group of MDAs clustering around an early Pliensbachian age between 192.9 and 189 Ma (BLC-01: 192.2 ± 6.1; MTY-02: 191.3 ± 1.8; RMK-01: 191.1 ± 3.6; WTK-03:189.1 ± 1.3). Samples from the upper zone reveal a collection of MDAs of early Toarcian age between 184.2 and 181 Ma (RMK-03: 181.3 ± 3.7; LKP-01: 182.0 ± 2.5; BLC-03: 183.4 ± 4.3; MKY-03; 183.5 ± 5.6, BLC-02: 184.0 ± 3.1). Preferred MDAs with a clustering of middle to late Pliensbachian age (189 to 185) are also present (LKP-02: 188.7: ± 1.9; KMB-03: 187.6 ± 2.6). Samples from Leeuwkop (LKP 1–3) present an age reversal, where the sample from the middle zone is older than the sample from the upper zone. It is noted that samples with meaningful MDA results were mostly from the south of the basin.

6 | DISCUSSION

6.1 | Provenance of detrital grains

Interpreting the origin of sediment grains requires cautious consideration, as diagenetic dissolution may introduce bias, potentially distorting the signal of the true sediment origin in favour of stable to ultra-stable heavy minerals (Garzanti, Andò, et al., 2018; Haughton et al., 1991; Milliken, 1988; Morton, 1984, 1985). Diagenetic dissolution can cause a very uniform heavy mineral suite by diagenetic modification of detritus because burial promotes the selective survival of ultra-stable minerals, such as ZTR. Additionally, sediments sourced from mostly recycled sedimentary sources will also result in a lack of diversity in heavy mineral suites. These heavy mineral trends are generally retained for detritus reworked into a new sedimentary basin (Garzanti, 2017; Garzanti et al., 2013; Garzanti, Andò, et al., 2018; Johnsson & Basu, 1993). Given the limited burial (1500–2000 m) of the Clarens Formation (Svensen et al., 2008), the dominance of ultra-stable ZTR heavy minerals in samples examined petrographically in this current study, along with the homogenous heavy

13652117, 2024, 3, Downloaded from https://onlinelibrary.wiley.com/doi/10.1111/bre.12877 by South African Medical Research, Wiley Online Library on [14/06/2024]. See the Terms and Conditions (https://onlinelibrary.wiley.com/terms-and-conditions) on Wiley Online Library for rules of use; OA articles are governed by the applicable Creative Commons License

TABLE 1 Maximum depositional ages (MDAs) of the Clarens Formation using the youngest single grain (YSG) and 2 or more clustered dates (YC2s[+2]). For location and stratigraphic position, see Figures 2 and 3. See text for details. Uncertainty of 2 SE represents propagated uncertainty using iolite (Paton et al., 2010).

	Preferred		YSG		Cluster (2+2s)				
	Age	2s	Age	2s	Age	2s	No. of dates	MSWD	Discordance range (%)
RMK-03	181.3	3.7	181.3	3.7	201.4	2.8	2	0.97	0–2
LKP-01	182.0	2.5	180.8	3.5	182.0	2.5	2	1.1	0–2
BLC-03	183.4	4.3	183.1	6.8	183.4	4.3	2	0.055	0–1
MKY-03	183.5	5.6	183.5	5.6	237.8	2.2	6	2.1	0–2
BLC-02	184.3	3.1	183.4	5.1	184.3	3.1	2	0.092	0–3
KMB-03	187.6	2.6	187.6	2.6	259.2	2.4	2	4.3	0–2
LKP-02	188.7	1.9	185.5	4.7	188.7	1.9	4	2.1	0–2
WTK-03	189.1	1.3	187.1	1.9	189.1	1.3	2	4.8	0–1
MTY-02	191.3	1.8	189.5	3.8	191.3	1.8	3	1.4	0–2
RMK-01	191.1	3.6	191.1	3.6	193.4	2.4	2	2.3	0–1
BLC-01	192.2	6.1	192.2	6.1	197.5	1.7	9	1.5	0–3
MTY-03	—	—	178.1	2.8	211.0	2.0	2	2.5	0–1
LKP-03	—	—	202.1	4.3	225.1	2.8	2	2.0	0–1
KMB-02	—	—	215.3	3.2	247.6	2.4	2	0.96	0–2
MKY-02	—	—	241.1	4	242.4	2.3	3	0.47	0–3
RMK-02	—	—	247.3	5.1	251.9	3.4	2	7.7	0–1
WTK-02	—	—	238.8	2.7	254.2	2.3	2	1.6	0–1
KMB-01	—	—	200.1	2.4	537.1	2.3	6	1.8	0–1
MKY-01	—	—	208.7	3.4	245.7	2.2	5	2.1	0–2
MTY-01	—	—	209.6	4.1	273.1	2.2	4	1.9	0–3
WTK-01	—	—	228.7	2.7	246.3	1.9	2	0.4	0–3

mineral suite, a strong recycled component was likely incorporated into the sediments. Conversely, the uniform nature of the sandstone compositions may point towards sediment homogenisation (Bertolini et al., 2020; Garzanti, 2016; Garzanti et al., 2006, 2014; Garzanti, Andò, et al., 2018; Morton & Hallsworth, 2007; Weltje & von Eynatten, 2004). Unstable minerals, like epidote, hornblende and titanite, in the Clarens Formation furthermore indicate the supply of sediment from primary sources. Also, the presence of these unstable minerals, particularly hornblende, supports the idea of relatively shallow burial depths (1500–1700 m) since amphiboles are considered unstable under deeper burial conditions (Garzanti, Andò, et al., 2018; Morton & Hallsworth, 2007). The absence of dissolution textures in detrital garnet grains likewise suggests relatively shallow burial as garnet typically survives up to about 2000 m in depth due to its moderate stability (Ando et al., 2012).

The dominance of monocrystalline quartz in the Clarens Formation aligns with its well-established aeolian nature and suggests a recycled assemblage (Blatt & Christie, 1963; Garzanti et al., 2013; Muhs, 2004). In contrast, the localized occurrence of polycrystalline quartz along the eastern edge of the basin could point to a primary source in this area (Basu, 1985; Basu et al., 1975). Furthermore, polycrystalline quartz grains consisting of four or more interlocking crystals are also suggestive of primary plutonic igneous or high-grade metamorphic sources (Basu, 1985; Basu et al., 1975). Given the localized occurrence of ephemeral fluvial deposits along the eastern edge of the basin (Head, 2022; Head & Bordy, 2023a, 2023b), this metamorphic source would have been situated to the east of the basin. Epidote and amphibole along with garnet in the samples strengthen the argument for a metamorphic basement source, as these minerals are associated with regional metamorphic terrains (Garzanti et al., 2007; Schneider et al., 2016).

The medium- to very fine-grained sandstones are typical of aeolian transported sand, where silty and sandy silt represent dust fall processes (Head, 2022; Head & Bordy, 2023b). The rounding trend is related to abrasion during aeolian transport, which results in the breakage and chipping of large grains into smaller grains that tend to be more angular. Typically, quartz dominates desert

13652117, 2024, 3, Downloaded from https://onlinelibrary.wiley.com/doi/10.1111/bre.12877 by South African Medical Research, Wiley Online Library on [14/06/2024]. See the Terms and Conditions (https://onlinelibrary.wiley.com/terms-and-conditions) on Wiley Online Library for rules of use; OA articles are governed by the applicable Creative Commons License

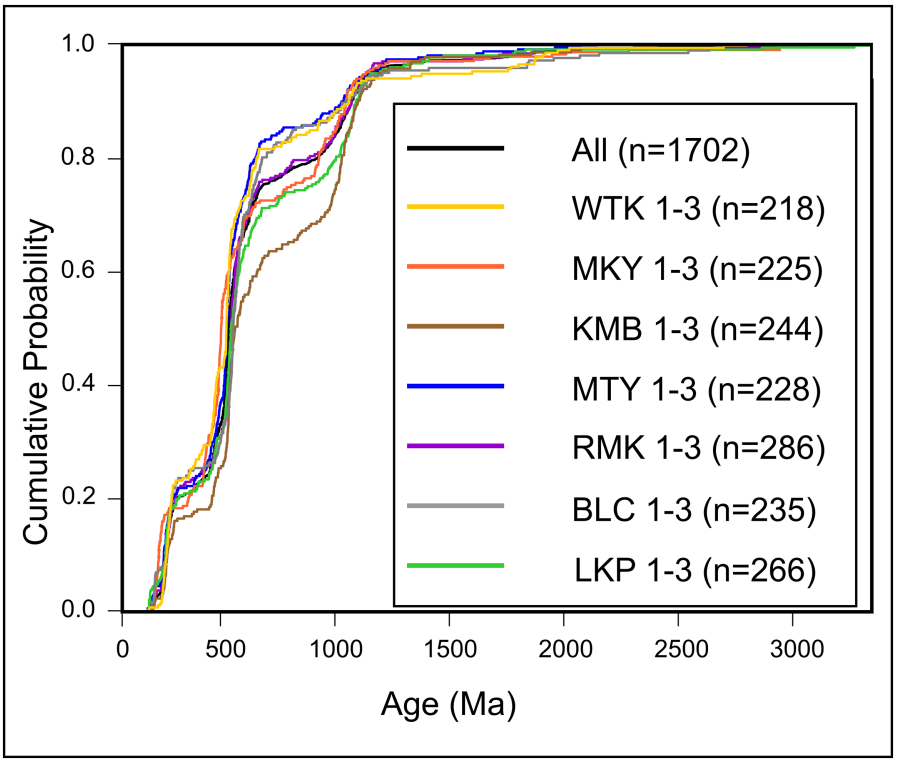


FIGURE 10 Cumulative probability plots for all samples combined and grouped per sample location.

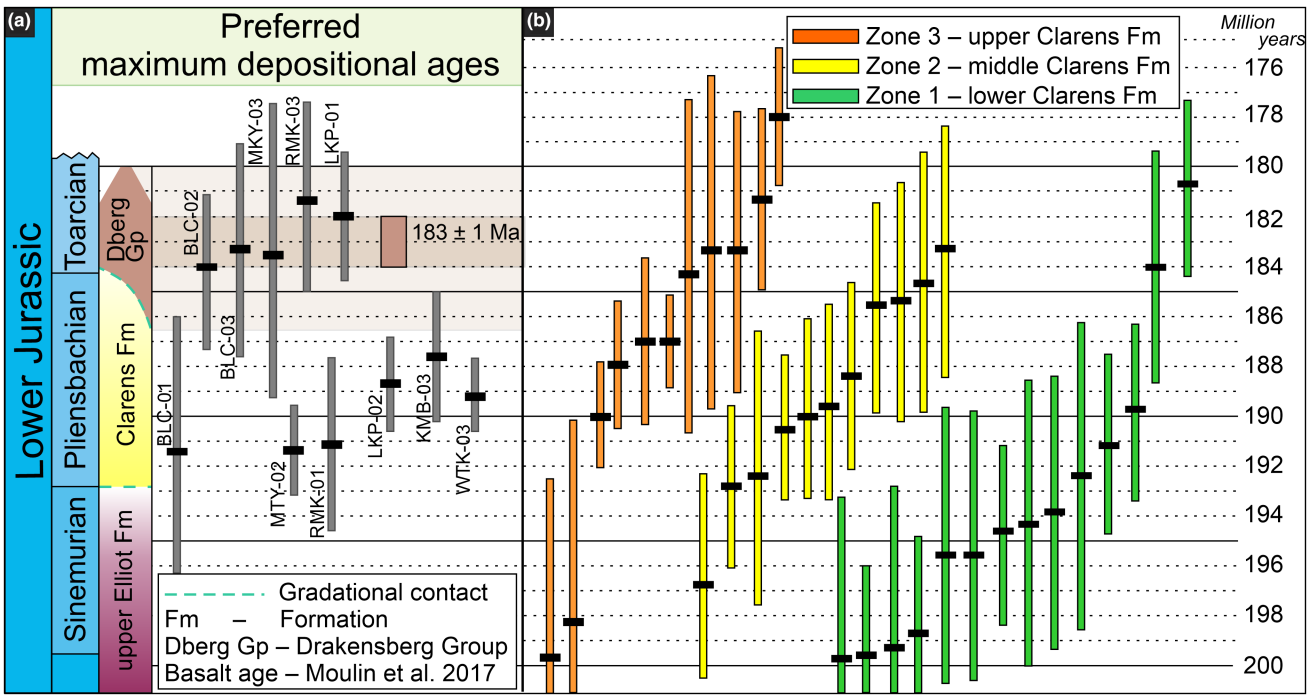


FIGURE 11 Detrital zircon geochronology of the Clarens Formation. (a) Preferred maximum depositional ages. (b) Distribution of all zircon dates younger than 200 Ma. Zones are lithostratigraphic intervals as defined by Beukes (1969, 1970) and refined by Head (2022). Bar heights (yellow, green, orange, and grey) depict 2 SE uncertainty. In addition to Moulin et al. (2017), the 183 ± 1 Ma age of the Drakensberg Group is also based on Duncan et al. (1997) and Svensen et al. (2012).

13652117, 2024, 3, Downloaded from https://onlinelibrary.wiley.com/doi/10.1111/bre.12877 by South African Medical Research, Wiley Online Library on [14/06/2024]. See the Terms and Conditions (https://onlinelibrary.wiley.com/terms-and-conditions) on Wiley Online Library for rules of use; OA articles are governed by the applicable Creative Commons License

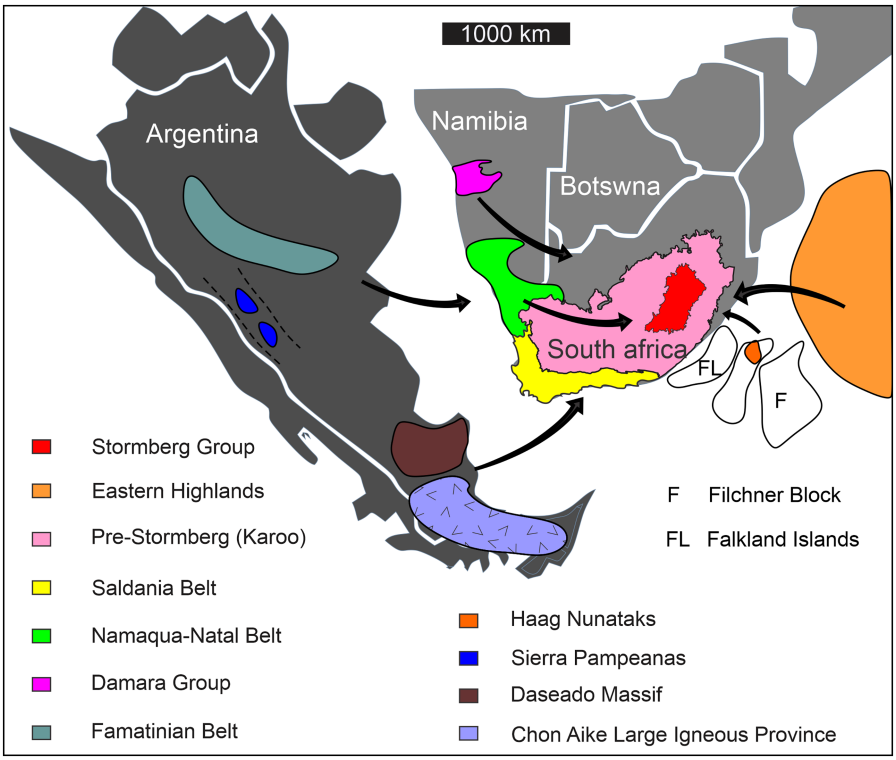


FIGURE 12 Source rock distribution of the Clarens Formation in southern Gondwana during the Early Jurassic (map compiled and modified after Bial et al., 2015; Bordy & Head, 2018; Casquet et al., 2008; Foster et al., 2015; Frimmel et al., 2013; Jacobs et al., 2008; Muir et al., 2020; Pankhurst et al., 2000; Pankhurst et al., 2006 and Ryan & Whitfield, 1979).

sediments because of its mechanical and chemical stability and the availability of recycled quartz sources (Garzanti, 2019; Muhs, 2004). This results in a pure quartzose (qQ) being very common in areas dominated by ancient aeolian processes. However, the slightly higher feldspar content, in addition to the dominance of quartzose (Q) samples in the Clarens Formation, may reflect a granitic basement exposed in the proximity, such as is the case for dunes in western Egypt and the Sinai Desert (Grarzanti, 2019). This granitic source may have been in the Kaapvaal Craton and also within the Cape Fold Belt (e.g., Bordy et al., 2004; Johnsson et al., 2006; Rust, 1967). A similar feldspar content for the underlying upper Elliot Formation was reported by Bordy et al. (2004), who attributed the feldspar increase across the Triassic–Jurassic boundary to crustal-scale faults that exposed basement rocks along the western margin of the MKB in the earliest Jurassic (Hettangian–Sinemurian; Bordy et al., 2004, 2005; Bordy, Abrahams, et al., 2020). This proximal basement source may have persisted during the deposition of the conformably overlying Clarens Formation. Alternatively, increased feldspar can be linked to the aridification trend in the Stormberg Group (Bordy et al., 2004, 2021; Bordy, Abrahams, et al., 2020; Bordy, Rampersadh, et al., 2020).

The general lack of lithics in the Clarens Formation suggests that sediments were mostly sourced from the west as part of the dominant, compositionally more mature aeolian detritus that represent distal sources. In this context, localised occurrences of polycrystalline quartz grains with sutured contacts and more than four crystals per grain may be representative of a low-rank metamorphic source (Basu, 1985; Basu et al., 1975). The occurrence of these grains in fluvial deposits with palaeo-current flow towards the west and northwest (Eriksson, 1979, 1981, 1986) supports the argument for a distinct source terrain in the east. For example, this source could have been the "Eastern Highlands" (Ryan & Whitfield, 1979) and the western Antarctic Haag Nunataks terrain that was likely situated to the southeast of the basin (Jacobs et al., 2008; Jordan et al., 2020; Rino et al., 2008). Finally, the occurrence of rare mafic volcanic lithic fragments in the uppermost Clarens Formation at Talon (Figure 6c) may indicate the incorporation of primary volcanic material, further supporting the idea of an earlier onset of basaltic volcanism in the southern part of the Clarens basin relative to the north (see below and Bordy et al., 2021; Moulin et al., 2017).

6.2 | Detrital zircon provenance

The most abundant detrital zircon grains reflect dates that are consistent with a Cambrian to Early Neoproterozoic

13652117, 2024, 3, Downloaded from https://onlinelibrary.wiley.com/doi/10.1111/bre.12877 by South African Medical Research, Wiley Online Library on [14/06/2024]. See the Terms and Conditions (https://onlinelibrary.wiley.com/terms-and-conditions) on Wiley Online Library for rules of use; OA articles are governed by the applicable Creative Commons License

(Pan-African) age fraction that can be linked to the Damara and Saldania belts during the formation of Gondwana (Figure 12; Foster et al., 2015; Frimmel et al., 2013; Rino et al., 2008). The Damara Belt consist of basal coarse clastic sedimentary rocks of the Nosib Group, which is overlain by meta-turbidites and other metasedimentary successions of the Swakop Group (Foster et al., 2015) with a zircon age fraction of 600–900 Ma, specifically in the northern part. The Saldania Belt comprises siliciclastic and minor carbonate sedimentary rocks with a low-grade metamorphic overprint (Frimmel et al., 2013) and an age range of 532–609 Ma in the Boland Zone. Similar prominent Cambrian to Early Neoproterozoic (Pan-African) ages have been identified in the Karoo Supergroup of southwestern Gondwana (Figure 12), such as the Beaufort Group in the MKB (Viglietti et al., 2018), the Botucatu Formation in Brazil (Pinto et al., 2015), the Etjo Formation in Namibia (Zieger et al., 2020), and Karoo correlatives in the Congo Basin (Linol et al., 2016). A Tonian to Stenian (Grenvillian) age fraction is the second most abundant, and sedimentary source terranes with this age range can be attributed to the genesis of the Namaqua-Natal Mobile Belt (Figure 12; Bial et al., 2015: 1350–1100 Ma) and the western Sierras Pampeanas (Rapela et al., 2010: 1330–1030 Ma). These metasedimentary sequences are part of the Grenvillian orogen of western Gondwana, with a prominent age peak between 1.0 and 1.2 Ga (Figure 12; Casquet et al., 2006, 2008; Rino et al., 2008; Rapela et al., 2010).

A Permian age fraction represents a significant part of the age population (up to 19% in some samples) in the Clarens Formation. Euhedral zircons of Permian age described by Viglietti et al. (2018) from the MKB have been interpreted as primary ashfall zircons, whereas zircons from the Clarens Formation with this age fraction show moderate rounding. This feature may indicate that the incorporation of Permian age fractions in the detritus of the Clarens Formation records recycling from older Karoo sedimentary rocks, particularly the Permo-Triassic Beaufort Group. A similar Permian age fraction has also been identified in the zircon age distributions of the Lower Jurassic Etjo Formation in Namibia (Zieger et al., 2020). The Ordovician age fraction present in the Clarens Formation is interpreted to be linked to the Deseado Massif (Bowden, 2014) or the Famatinian Belt of the eastern Sierras Pampeanas (Pankhurst et al., 2006; Rapela et al., 2010: Early to Middle Ordovician 490–470 Ma), whereas rare mid-Palaeoproterozoic and Archean age fractions may reflect a source terrain of either the Orange River Group or the Richtersveld Magmatic Arc within the Namaqua Sector (Hofmann et al., 2014; Macey et al., 2017; Minnaar, 2011; Zieger et al., 2020: 1910–1865 Ma) or the Transvaal Supergroup and Kheis Subprovince (Van Niekerk, 2006; Viglietti et al., 2018; Zieger et al., 2020: 1800–2700 Ma).

An Early Jurassic detrital zircon age fraction (192.2 ± 6.1 Ma to 181.3 ± 3.7 Ma) may represent a reworked primary source. Ash beds in the Suurberg Group of South Africa providing zircon dates of similar age likely reflect Early Jurassic volcanism in Patagonia and the Antarctic Peninsula (Muir et al., 2020). This volcanism was associated with the Chon Aike Magmatic Province of the southwest of Gondwana, where a major pulse in the active arc magmatism occurred between ~188 and 178 Ma, after a period of magmatic quiescence (~200–188 Ma; Bastias et al., 2021; Cúneo et al., 2013; Féraud et al., 1999; Muir et al., 2020: their figure 11; Pankhurst et al., 1998; Pol et al., 2020). It is therefore inferred that pyroclastic ash plumes having originated from this active volcanic region were subsequently windswept towards the various Early Jurassic basins. Based on position and age, this source may therefore have contributed to the Early Jurassic zircon age fraction incorporated into the detritus of the Clarens Formation.

In all samples of the Clarens Formation, the provenance reflects a major contribution from a Cambrian to an Early Neoproterozoic (Pan-African) source. In the context of the potential source areas to the Clarens Formation, Cambrian to Early Neoproterozoic (Pan-African) zircons are reflective of tectonic activity related to the assembly of Gondwana (Foster et al., 2015; Frimmel et al., 2013; Konopásek et al., 2017), whereas Tonian-Stenian (Grenvillian) zircon age fractions are associated with the assembly of Rodinia (Bial et al., 2015; Casquet et al., 2008; Rapela et al., 2010; Rino et al., 2008; Van Kranendonk & Kirkland, 2013). However, a unique sample is identified in the Kamberg area (KMB-01), where the basal sample has a significant contribution from a Tonian-Stenian (Grenvillian) age component. This is further evidenced by the cumulative probability plots that indicate a difference in the spread of the Kamberg zircon dates (Figure 10), the presence of coarser sandstones that are often gritty in places and the abundant appearance of polycrystalline quartz in this part of the succession. The basal Clarens Formation of the Kamberg area is interpreted as fluvial channel deposits (Eriksson, 1981, 1986; Head, 2022) with palaeo-flow directions towards the southwest, indicating a localized sediment source terrain in the northeast to east. Given the Early Jurassic palaeogeography of Gondwana and a persistent sediment supply from the east throughout the evolution of the MKB, a long-lived Antarctic sediment source area (the "Eastern Highlands") can be inferred for the Clarens Formation as well (e.g., Bordy & Prevec, 2008; Ryan & Whitfield, 1979). Moreover, the western Antarctic Haag Nunataks (1170–1060 Ma) may also be regarded as a possible source for this localized part of the succession (Jacobs et al., 2008; Jordan et al., 2020; Rino et al., 2008).

13652117, 2024, 3, Downloaded from https://onlinelibrary.wiley.com/doi/10.1111/bre.12877 by South African Medical Research, Wiley Online Library on [14/06/2024]. See the Terms and Conditions (https://onlinelibrary.wiley.com/terms-and-conditions) on Wiley Online Library for rules of use; OA articles are governed by the applicable Creative Commons License

6.3 | A revised chronostratigraphic framework for the Clarens Formation

Overall, the Clarens Formation reflects a depositional history of ~10 Ma throughout the Pliensbachian into the early Toarcian, when deposition was partially synchronous with but ultimately ending by the outpouring of the Karoo continental flood basalts (Moulin et al., 2017). More specifically, the preferred MDAs of the samples from the Clarens Formation suggest two meaningful age ranges (Figure 11, Table 1). Firstly, the basal and middle samples (Zones 1 and 2) indicate a cluster of MDAs in the Pliensbachian and suggest that the basal Clarens Formation may be of early Pliensbachian age or younger (~191–192 Ma). A second cluster is also apparent in the early Toarcian, demonstrating that the upper Clarens Formation may be of early Toarcian age or younger (~181–183 Ma). These detrital zircon age trends are deemed chrono-stratigraphically significant given the existing geochronological constraints of the Clarens Formation, such as biostratigraphy (Knoll, 2005; Viglietti et al., 2020), published MDAs (Bordy, Abrahams, et al., 2020; Bordy, Rampersadh, et al., 2020) and crystallization ages of igneous rocks in the Drakensberg Group (Duncan et al., 1997; Moulin et al., 2017; Svensen et al., 2012). Additionally, Clarens Formation U–Pb zircon ages from the Springbok Flats area north of the MKB (MDA of 187 ± 1.6 Ma; Nxumalo, 2020) and from the lower Clarens Formation in the southern MKB (MDA of 187.5 ± 1.6 Ma; Bordy, Abrahams, et al., 2020; Bordy, Rampersadh, et al., 2020) have also been reported. Despite the presence of this middle to late Pliensbachian maximum depositional age, the overlapping uncertainty within the basal and upper MDA results cannot resolve this age as a distinct age fraction for the middle stratigraphic interval (middle zone of Beukes, 1969, 1970) of the Clarens Formation.

The current study provides a broad chronostratigraphic framework for the Clarens Formation, with two meaningful age fractions being associated with its lower and upper parts, particularly in the south of the basin. These are (1) An early Pliensbachian or younger age fraction for the basal Clarens Formation, also identified in its transitional lower contact with the upper Elliot Formation (Bordy, Abrahams, et al., 2020; Bordy, Rampersadh, et al., 2020; Bordy et al., 2021) and (2) an early Toarcian age fraction for the upper Clarens Formation. The MDAs reflect sediment supply dynamics related to a source that was largely contemporaneous with the deposition of the Clarens Formation, which might have been volcanic eruptions in the Chon Aike Magmatic Province (i.e., supplying primary ashfall zircons; Muir et al., 2020). It is noted that several samples yielded pre-Jurassic MDAs, and thus are older than the existing chronostratigraphic constraints (see Head, 2022, for details). These 'old' zircon crystals were likely sourced from pre-existing rocks, and thus are unhelpful for constraining the timing of Clarens deposition because they cannot be reconciled with existing multidisciplinary age data for the MKB. Consequently, we contend that the robust and sound geological evidence, particularly from the conformably overlying Drakensberg Group igneous rocks, at least for now, should take precedence. We regard the results from this study as a springboard for a more systematic geochronological work, which may include lower temperature chronometers as detrital proxies (rutile) or more precise dating techniques such as CA-ID-TIMS to further refine the current MDAs. This may enhance our understanding not only of the true depositional age of the Clarens Formation but also the dynamics of this vast Early Jurassic Gondwanan/Pangean erg, the spatio-temporal relationship of the northern and the southern facies in the MKB as well as the validity of the middle to late Pliensbachian age for the middle stratigraphic interval ('zone 2' of Beukes, 1970) of the Clarens Formation.

6.4 | Palaeogeographical implications

Detritus within the cover successions of southern Africa has been shown to consist largely of recycled sedimentary rocks (Figure 12; Andersen, Kristoffersen, et al., 2016; Andersen, Elburg, et al., 2016; Vorster, 2014), and this feature is strongly echoed by the Clarens Formation as evidenced by high ZTR abundance in the heavy minerals assemblages, a lack of variation in the heavy mineral suite, a high degree of rounding of zircon grains and zircon age fractions similar to those in older successions of the Karoo Supergroup and Pan-African (Cambrian to Early Neoproterozoic) aged successions (Andersen, Kristoffersen, et al., 2016; Andersen, Elburg, et al., 2016; Bordy, Abrahams, et al., 2020; Viglietti et al., 2018). When comparing the zircon populations from the Clarens Formation to that in the Beaufort Group (Viglietti et al., 2018), a strong similarity is evident, although the proportions of each zircon age population are different. While the dominant zircon age fraction is of Cambrian to Early Neoproterozoic (Pan-African) in the Clarens Formations, the Beaufort Group is characterized by a dominant zircon age fraction from the Permian (Viglietti et al., 2018). This similarity suggests that the Beaufort Group may have been a sediment source for the Clarens Formation, albeit only a partial one, as a shift to a dominant Pan-African source is observed. This, in turn, could indicate a larger input from the Damara and Saldania Orogenic Belts and a change in source dynamics relative to the pre-Stormberg successions (Figure 1b) by the Early Jurassic. This reworking of older Karoo strata during the

13652117, 2024, 3, Downloaded from https://onlinelibrary.wiley.com/doi/10.1111/bre.12877 by South African Medical Research, Wiley Online Library on [14/06/2024]. See the Terms and Conditions (https://onlinelibrary.wiley.com/terms-and-conditions) on Wiley Online Library for rules of use; OA articles are governed by the applicable Creative Commons License

deposition of the Clarens Formation was also envisaged by Beukes (1969, 1970), Eriksson (1986) and Eriksson et al. (1994), and is in line with the sediment recycling model of pre-Stormberg successions in the final stages of the Karoo foreland basin evolution (Bordy et al., 2004, 2005; Catuneanu et al., 1998).

Comparing zircon data from unpublished theses and publications pertinent to the Clarens Formation and equivalents throughout southern Africa to the dataset of this study, a broad similarity in age patterns is revealed, although with slight variations in proportions. Additional zircon data include one sample each from Bordy, Abrahams, et al. (2020) and Bordy, Rampersadh, et al. (2020); UMC in MKB: Clarens Formation, Rademan (2018; Map 6 in MKB: Clarens Formation), Nxumalo (2020; BK-1-1 in Springbok Flats Basin: Clarens Formation) and Zieger et al. (2020; NAM349 in Namibia: Etjo Formation), respectively. A similar source terrain for the Elliot and Clarens formations was suggested based on the heavy mineral assemblages and is observed in the MKB realm A of Zieger et al., 2020–see their figure 11. This trend is supported by the change in source dynamics for the upper Elliot Formation, where a west-to-east source input is reported to have occurred in the Early Jurassic (Bordy et al., 2004; Bordy, Abrahams, et al., 2020). Using statistical dissimilarity calculations, Zieger et al. (2020) determined that a common recycling history existed in the Late Triassic and Early Jurassic in southwestern Gondwana, and this may suggest a similar source terrain for the aeolianites across southern Africa in the Early Jurassic. Furthermore, the similarity of the sandstone compositions and the provenance age fractions in both the massive and large-scale cross-bedded facies (as discussed by Head & Bordy, 2023a, 2023b) further suggests that these facies were derived from the same source and that the downwind transitional deposits to sandy loess and loess may have been sourced from the upwind dunes, which in turn is suggestive of large-scale homogenisation of the sediments of the Clarens Formation and other regional Early Jurassic aeolianites.

The presence of a primary crystalline source is indicated by the unstable minerals in the heavy mineral suite throughout the Clarens Formation and the appearance of a small percentage of polycrystalline quartz along the eastern edge of the basin. This combination points to a primary metamorphic source. However, the extensive evidence for a high degree of recycled material incorporated into the detritus of the Clarens Formation shows that primary source inputs were obscured by the overwhelming input of recycled material. Therefore, meaningful conclusions regarding the source rock types and their precise locations are masked by the syn-sedimentary homogenisation of the sediments. Spatial variation in the source areas is lacking, except for a localized occurrence of fluvial deposits that contain polycrystalline quartz and a prominent Tonian–Stenian (Grenvillian) detrital age fraction, consistent with a likely source within the "Eastern Highlands" (now part of Antarctica; Figure 12).

Overall, the Clarens Formation captures the depositional dynamics in a vast palaeo-desert system that was active over southwestern Gondwana from the Pliensbachian to Early Toarcian. It also records an extensive sediment recycling history, where zircons were sourced from pre-existing Karoo deposits and the Damara and Saldania Mobile Belts along with the Namaqua-Natal Mobile Belt as well as the western Sierras Pampeanas. It also shows evidence of the large-scale homogenisation of detritus as sediments migrated towards the basin. Simultaneously, volcanic ash plumes from the Chon Aike Magmatic Province carried Early Jurassic zircon grains into the basin, establishing a geochronological framework with distinct upper and lower age boundaries for the Clarens Formation. The active aeolian system in this part of southwestern Gondwana was ultimately shut down by large-scale outpouring of continental flood basalts (Drakensberg Group) associated with the Karoo-Ferrar Large Igneous Province during the early Toarcian.

7 | CONCLUSION

Previous provenance studies of the Clarens Formation, a remnant of the early Mesozoic Pangean erg systems, have largely focused on its petrographic characterization. Zircon geochronology significantly complements sandstone petrography by unravelling not only the source areas but also the tempo of sediment supply during deposition. The combination of zircon geochronology and petrographic examination shows that the Clarens Formation detritus was recycled mainly from pre-existing sedimentary successions within and outside the MKB. Evidence includes high modal abundances of ZTR minerals, the lack of a diverse heavy mineral suite and the dominance of zircon populations that can be linked to large-scale tectonic events, particularly a Pan-African (Cambrian to Early Neoproterozoic) age fraction (490–650 Ma). The major source areas include the Damara and Saldania Orogenic belts, whereas minor sources can be linked to the Namaqua-Natal Mobile Belt and the western Sierras Pampeanas, both providing Grenvillian (Tonian–Stenian) zircon age fractions (0.9–1.1 Ga). Although the strongly recycled nature of the Clarens Formation detritus complicates many aspects of the provenance history, a primary source is inferred from the appearance of unstable heavy minerals and the higher feldspar content as compared to the sandstone composition of both modern and ancient desert systems. Localised provenance

13652117, 2024, 3, Downloaded from https://onlinelibrary.wiley.com/doi/10.1111/bre.12877 by South African Medical Research, Wiley Online Library on [14/06/2024]. See the Terms and Conditions (https://onlinelibrary.wiley.com/terms-and-conditions) on Wiley Online Library for rules of use; OA articles are governed by the applicable Creative Commons License

variations are only seen in the eastern part of the basin, where polycrystalline quartz is abundant and a prominent Grenvillian (Tonian–Stenian) age fraction is associated with sedimentary facies interpreted to have been sourced east of the MKB. Early Jurassic zircon ages appear throughout the Clarens Formation in the form of euhedral to slightly rounded sediment grains. The source for these Jurassic detrital zircon crystals is interpreted as pyroclastic ash plumes that originated from Early Jurassic volcanoes in Patagonia and Antarctica (Chon Aike Magmatic Province). This volcanic source has been identified in other early Mesozoic sedimentary successions of southern Gondwana, including southern Africa. The MDA calculations for detrital zircon crystals in the Clarens Formation refine its chrono-stratigraphic framework and show that the bulk of the Clarens Formation was deposited in the Pliensbachian and early Toarcian. More specifically, the lower part of the formation is of early Pliensbachian age or younger (~191–192) and the upper part, especially in the southern MKB, is of early Toarcian age or younger (~181–183 Ma). Future work should focus on analysing larger detrital datasets from the Clarens Formation and its counterparts across southern Africa to refine the depositional history and basin dynamics within and beyond the MKB as well as using more precise dating techniques, such as CA-ID-TIMS, to ascertain whether the middle Clarens Formation is middle to late Pliensbachian in age.

ACKNOWLEDGEMENTS

We are grateful for the field assistance and enthusiasm of Miengah Abrahams, Akhil Rampersadh, Yambi Dinis, Riyaad Mukaddam and Lara Sciscio. We are also grateful for support from the thin section lab of the UCT Department of Geological Sciences, as well as Marelli Grobbelaar at the SU CAF facility for help with zircon sample preparation. We thank Dr. Laura Bracciali (LB) for significant contributions during earlier stages of manuscript preparation, through the provision of a large amount of geochronological data and some interpretation. Her useful comments assisted greatly in improving the manuscript's structure, some of the writing and a few figures, elements of the sandstone petrography and provenance interpretation. While we appreciate Dr. Bracciali's expertise and insights, she cannot be held accountable for flaws or inadequacies related to the accuracy or integrity of this work. Instead, the authors accept full accountability for the content of the manuscript. We thank two anonymous reviewers, Trystan Herriott and editor Cari Johnson for their comprehensive and constructive feedback and efficient manuscript handling.

FUNDING INFORMATION

Support for this research came from grants obtained by EB from the South Africa's National Research Foundation (NRF—South Africa) Programme for Rated Researchers (CPRR) and African Origins Programme (AOP) (grant numbers 93544, 113394, 98825) along with grants from GENUS (DSI-NRF Centre of Excellence in Palaeosciences) (grant number UID 86073: 2019, 2020, 2021). Additional research support to HH was provided by the Geological Society of South Africa's (GSSA) REI Fund, a Palaeontological Trust (PAST) student research grant, a Society for Sedimentary Geology (SEPM) student grant and the Geological Society of America's GSA El-Baz student grant. Postgraduate bursary support to HH was received from both GENUS (DSI-NRF Centre of Excellence in Palaeosciences, UID 86073″ 2020, 2021, 2022) and the University of Cape Town (UCT Vice-Chancellor Scholarship – 2019, 2020). RB acknowledges financial support through an NRF-NEP grant (UID 105674) to establish the LA-SF-ICP-MS facility at the School of Geosciences, University of the Witwatersrand.

CONFLICT OF INTEREST STATEMENT

The authors declare that they have no known competing financial interests or personal relationships that could have appeared to influence the work reported in this article.

PEER REVIEW

The peer review history for this article is available at https://www.webofscience.com/api/gateway/wos/peer-review/10.1111/bre.12877.

DATA AVAILABILITY STATEMENT

Datasets generated and used in this study have been included in the article with supplementary material and data tables available at: https://figshare.com/s/6788ee86634ce85c9009 (doi: 10.6084/m9.figshare.19801978).

ORCID

Howard V. Head https://orcid.org/0000-0002-4808-7104

REFERENCES

Abrahams, M. (2020). Evaluation of tridactyl theropod tracks in southern Africa: Quantitative morphometric analysis across the Triassic–Jurassic boundary. Unpublished doctoral thesis, University of Cape Town http://hdl.handle.net/11427/32436

Abrahams, M., Bordy, E. M., & Knoll, F. (2021). Hidden for one hundred years: A diverse theropod ichnoassemblage and cross-sectional tracks from the historic Early Jurassic Tsikoane ichnosite (Clarens formation, northern Lesotho, southern Africa). *Historical Biology*, *33*(10), 2504–2519. https://doi.org/10.1080/08912963.2020.1810681

13652117, 2024, 3, Downloaded from https://onlinelibrary.wiley.com/doi/10.1111/bre.12877 by South African Medical Research, Wiley Online Library on [14/06/2024]. See the Terms and Conditions (https://onlinelibrary.wiley.com/terms-and-conditions) on Wiley Online Library for rules of use; OA articles are governed by the applicable Creative Commons License

Andersen, T., Elburg, M., & Cawthorn-Blazeby, A. (2016). U–Pb and Lu–Hf zircon data in young sediments reflect sedimentary recycling in eastern South Africa. *Journal of the Geological Society*, *173*(2), 337–351. https://doi.org/10.1144/jgs2015-006

Andersen, T., Kristoffersen, M., & Elburg, M. A. (2016). How far can we trust provenance and crustal evolution information from detrital zircons? A South African case study. *Gondwana Research*, *34*, 129–148. https://doi.org/10.1016/j.gr.2016.03.003

Andò, S., Garzanti, E., Padoan, M., & Limonta, M. (2012). Corrosion of heavy minerals during weathering and diagenesis: A catalog for optical analysis. *Sedimentary Geology*, *280*, 165–178.

Bastias, J., Spikings, R., Riley, T., Ulianov, A., Grunow, A., Chiaradia, M., & Hervé, F. (2021). A revised interpretation of the Chon Aike magmatic province: Active margin origin and implications for the opening of the Weddell Sea. *Lithos*, *386*, 106013. https://doi.org/10.1016/j.lithos.2021.106013

Basu, A. (1985). Reading provenance from detrital quartz. In *Provenance of arenites* (pp. 231–247). Springer.

Basu, A., Young, S. W., Suttner, L. J., James, W. C., & Mack, G. H. (1975). Re-evaluation of the use of undulatory extinction and polycrystallinity in detrital quartz for provenance interpretation. *Journal of Sedimentary Research*, *45*(4), 873–882. https://doi.org/10.1306/212F6E6F-2B24-11D7-8648000102C1865D

Bertolini, G., Marques, J. C., Hartley, A. J., Da-Rosa, A. A., Scherer, C. M., Basei, M. A., & Frantz, J. C. (2020). Controls on Early Cretaceous desert sediment provenance in southwest Gondwana, Botucatu formation (Brazil and Uruguay). *Sedimentology*, *67*(5), 2672–2690. https://doi.org/10.1111/sed.12715

Beukes, N. J. (1969). Die sedimentologie van die Etage Holkranssandsteen, sisteem Karoo. Unpublished MSc dissertation, University of the Orange Free State, Bloemfontein, 138 pp http://hdl.handle.net/11660/7671

Beukes, N. J. (1970). Stratigraphy and sedimentology of the Cave Sandstone stage, Karoo system. In S. H. Haughton (Ed.), *Proceedings and papers of the 2nd Gondwana symposium* (pp. 321–341). Council for Scientific and Industrial Research.

Bial, J., Büttner, S. H., Schenk, V., & Appel, P. (2015). The long-term high-temperature history of the central Namaqua metamorphic complex: Evidence for a Mesoproterozoic continental back-arc in southern Africa. *Precambrian Research*, *268*, 243–278. https://doi.org/10.1016/j.precamres.2015.07.012

Blakey, R. C. (1988). Basin tectonics and erg response. *Sedimentary Geology*, *56*(1-4), 127–151.

Blatt, H., & Christie, J. M. (1963). Undulatory extinction in quartz of igneous and metamorphic rocks and its significance in provenance studies of sedimentary rocks. *Journal of Sedimentary Research*, *33*(3), 559–579. https://doi.org/10.1306/74D70EBB-2B21-11D7-8648000102C1865D

Bordy, E. M. (2008). Enigmatic trace fossils from the aeolian lower Jurassic Clarens Formation, southern Africa. *Palaeontologia Electronica*, *11*, 16A.

Bordy, E. M., Abrahams, M., Sharman, G. R., Viglietti, P. A., Benson, R. B., McPhee, B. W., Barrett, P. M., Sciscio, L., Condon, D., Mundil, R., & Rademan, Z. (2020). A chronostratigraphic framework for the upper Stormberg Group: Implications for the Triassic-Jurassic boundary in southern Africa. *Earth-Science Reviews*, *203*, 103120. https://doi.org/10.1016/j.earscirev.2020.103120

Bordy, E. M., Bumby, A. J., Catuneanu, O., & Eriksson, P. G. (2009). Possible trace fossils of putative termite origin in the lower Jurassic (Karoo Supergroup) of South Africa and Lesotho. *South African Journal of Science*, *105*(9–10), 356–362.

Bordy, E. M., & Catuneanu, O. (2002). Sedimentology and palaeontology of upper Karoo aeolian strata (Early Jurassic) in the Tuli Basin, South Africa. *Journal of African Earth Sciences*, *35*(2), 301–314. https://doi.org/10.1016/S0899-5362(02)00103-3

Bordy, E. M., Hancox, P. J., & Rubidge, B. S. (2004). Provenance study of the Late Triassic-Early Jurassic Elliot Formation, main Karoo Basin, South Africa. *South African Journal of Geology*, *107*(4), 587–602. https://doi.org/10.2113/gssajg.107.4.587

Bordy, E. M., Hancox, P. J., & Rubidge, B. S. (2005). The contact of the Molteno and Elliot formations through the main Karoo Basin, South Africa: A second-order sequence boundary. *South African Journal of Geology*, *108*, 351–364. https://doi.org/10.2113/108.3.351

Bordy, E. M., Haupt, T. N., & Head, H. V. (2021). Karoo lava-fed deltas and a petrified forest from the Lower Jurassic of southern Gondwana. *Palaeogeography, Palaeoclimatology, Palaeoecology*, *575*, 110484. https://doi.org/10.1016/j.palaeo.2021.110484

Bordy, E. M., & Head, H. V. (2018). Lithostratigraphy of the Clarens Formation (Stormberg Group, Karoo supergroup), South Africa. *South African Journal of Geology*, *121*(1), 119–130. https://doi.org/10.25131/sajg.121.0009

Bordy, E. M., Lockley, M. G., Rampersadh, A., Mukaddam, R., & Head, H. V. (2022). Life and land engulfed in the late Early Jurassic Karoo lavas of southern Gondwana. *Geological Magazine*, *160*(4), 645–666. https://doi.org/10.1017/S0016756822001169

Bordy, E. M., & Prevec, R. (2008). Sedimentology, palaeontology and palaeo-environments of the Middle (?) to Upper Permian Emakwezini Formation (Karoo Supergroup, South Africa). *South African Journal of Geology*, *111*, 429–458.

Bordy, E. M., Rampersadh, A., Abrahams, M., Lockley, M. G., & Head, H. V. (2020). Tracking the Pliensbachian–Toarcian Karoo firewalkers: Trackways of quadruped and biped dinosaurs and mammaliaforms. *PLoS One*, *15*(1), e0226847. https://doi.org/10.1371/journal.pone.0226847

Bowden, L. L. (2014). A comparative study of detrital zircon ages from river sediment and rocks of the Karoo Supergroup (Late Carboniferous to Jurassic), Eastern Cape Province, South Africa: Implications for the tectono-sedimentary evolution of Gondwanaland's southern continental margin. Unpublished doctoral thesis, University of Johannesburg.

Casquet, C., Pankhurst, R. J., Fanning, C. M., Baldo, E., Galindo, C., Rapela, C. W., González-Casado, J. M., & Dahlquist, J. A. (2006). U–Pb SHRIMP zircon dating of Grenvillian metamorphism in Western Sierras Pampeanas (Argentina): Correlation with the Arequipa-Antofalla craton and constraints on the extent of the Precordillera Terrane. *Gondwana Research*, *9*(4), 524–529.

Casquet, C., Pankhurst, R. J., Rapela, C. W., Galindo, C., Fanning, C. M., Chiaradia, M., Baldo, E., González-Casado, J. M., & Dahlquist, J. A. (2008). The Mesoproterozoic Maz terrane in the Western Sierras Pampeanas, Argentina, equivalent to the Arequipa–Antofalla block of southern Peru? Implications for West Gondwana margin evolution. *Gondwana Research*, *13*(2), 163–175.

Catuneanu, O., Hancox, P. J., & Rubidge, B. S. (1998). Reciprocal flexural behaviour and contrasting stratigraphies: A new basin

13652117, 2024, 3, Downloaded from https://onlinelibrary.wiley.com/doi/10.1111/bre.12877 by South African Medical Research, Wiley Online Library on [14/06/2024]. See the Terms and Conditions (https://onlinelibrary.wiley.com/terms-and-conditions) on Wiley Online Library for rules of use; OA articles are governed by the applicable Creative Commons License

development model for the Karoo retroarc foreland system, South Africa. *Basin Research*, *10*, 417–440. https://doi.org/10.1046/j.1365-2117.1998.00078.x

Catuneanu, O., Wopfner, H., Eriksson, P. G., Cairncross, B., Rubidge, B. S., Smith, R. M. H., & Hancox, P. J. (2005). The Karoo basins of south-Central Africa. *Journal of African Earth Sciences*, *43*, 211–253. https://doi.org/10.1016/j.jafrearsci.2005.07.007

Corfu, F., Hanchar, J. M., Hoskin, P. W., & Kinny, P. (2003). Atlas of zircon textures. *Reviews in Mineralogy and Geochemistry*, *53*(1), 469–500. https://doi.org/10.2113/0530469

Coutts, D. S., Matthews, W. A., & Hubbard, S. M. (2019). Assessment of widely used methods to derive depositional ages from detrital zircon populations. *Geoscience Frontiers*, *10*(4), 1421–1435. https://doi.org/10.1016/j.gsf.2018.11.002

Crook, K. A. (1960). Classification of arenites. *American Journal of Science*, *258*(6), 419–428.

Cúneo, R., Ramezani, J., Scasso, R., Pol, D., Escapa, I., Zavattieri, A. M., & Bowring, S. A. (2013). High-precision U–Pb geochronology and a new chronostratigraphy for the Cañadón Asfalto Basin, Chubut, central Patagonia: Implications for terrestrial faunal and floral evolution in Jurassic. *Gondwana Research*, *24*(3–4), 1267–1275.

Dickinson, W. R. (1985). Interpreting provenance relations from detrital modes of sandstones. In *Provenance of arenites* (pp. 333–361). Springer Netherlands.

Dickinson, W. R., & Gehrels, G. E. (2003). U–Pb ages of detrital zircons from Permian and Jurassic eolian sandstones of the Colorado Plateau, USA: Paleogeographic implications. *Sedimentary Geology*, *163*, 29–66.

Dickinson, W. R., & Gehrels, G. E. (2009). Use of U-Pb ages of detrital zircons to infer maximum depositional ages of strata: A test against a Colorado plateau Mesozoic database. *Earth and Planetary Science Letters*, *288*(1), 115–125. https://doi.org/10.1016/j.epsl.2009.09.013

du Toit, A. L. (1905). Geological survey of the division of Aliwal North, Herschel, Barkly East and part of Wodehouse. Annual Report of the Geological Commission of the Cape of Good Hope, 71–181.

du Toit, A. L. (1918). The zones of the Karroo system and their distribution. *Proceedings of the Geological Society of South Africa*, *21*, 17–36.

Duncan, R. A., Hooper, P. R., Rehacek, J., Marsh, J., & Duncan, A. R. (1997). The timing and duration of the Karoo igneous event, southern Gondwana. *Journal of Geophysical Research - Solid Earth*, *102*(B8), 18127–18138. https://doi.org/10.1029/97JB00972

Eriksson, P. G. (1979). Mesozoic sheetflow and playa sediments of the Clarens Formation in the Kamberg area of the Natal Drakensberg. *South African Journal of Geology*, *82*(2), 257–258.

Eriksson, P. G. (1981). A palaeoenvironmental analysis of the Clarens formation in the Natal Drakensberg. *Transactions Geological Society of South Africa*, *84*, 7–17.

Eriksson, P. G. (1986). Aeolian dune and alluvial fan deposits in the Clarens formation of the Natal Drakensberg. *Transactions Geological Society of South Africa*, *89*, 389–393.

Eriksson, P. G., McCourt, S., & Snyman, C. P. (1994). A note on the petrography of upper Karoo sandstones in the Natal Drakensberg: implications for the Clarens Formation palaeoenvironment. *South African Journal of Geology*, *97*(1), 101–106.

Féraud, G., Alric, V., Fornari, M., Bertrand, H., & Haller, M. (1999). $^{40}Ar/^{39}Ar$ dating of the Jurassic volcanic province of Patagonia: Migrating magmatism related to Gondwana break-up and subduction. *Earth and Planetary Science Letters*, *172*(1–2), 83–96. https://doi.org/10.1016/S0012-821X(99)00190-9

Folk, R. L. (1980). *Petrology of sedimentary rocks* (p. 182). Hemphill Publishing Company.

Foster, D. A., Goscombe, B. D., Newstead, B., Mapani, B., Mueller, P. A., Gregory, L. C., & Muvangua, E. (2015). U–Pb age and Lu–Hf isotopic data of detrital zircons from the neoproterozoic Damara Sequence: Implications for Congo and Kalahari before Gondwana. *Gondwana Research*, *28*(1), 179–190. https://doi.org/10.1016/j.gr.2014.04.011

Frimmel, H. E., Basei, M. A., Correa, V. X., & Mbangula, N. (2013). A new lithostratigraphic subdivision and geodynamic model for the pan-African western Saldania Belt, South Africa. *Precambrian Research*, *231*, 218–235. https://doi.org/10.1016/j.precamres.2013.03.014

Gärtner, A., Linnemann, U., Sagawe, A., Hofmann, M. U., & Kleber, A. (2013). Morphology of zircon crystal grains in sediments—Characteristics, classifications, definitions. *Geologica Saxonica*, *59*, 65–73.

Garzanti, E. (2016). From static to dynamic provenance analysis—Sedimentary petrology upgraded. *Sedimentary Geology*, *336*, 3–13.

Garzanti, E. (2017). The maturity myth in sedimentology and provenance analysis. *Journal of Sedimentary Research*, *87*(4), 353–365. https://doi.org/10.2110/jsr.2017.17

Garzanti, E. (2019). Petrographic classification of sand and sandstone. *Earth-Science Reviews*, *192*, 545–563. https://doi.org/10.1016/j.earscirev.2018.12.014

Garzanti, E., Andò, S., Limonta, M., Fielding, L., & Najman, Y. (2018). Diagenetic control on mineralogical suites in sand, silt, and mud (Cenozoic Nile Delta): Implications for provenance reconstructions. *Earth-Science Reviews*, *185*, 122–139. https://doi.org/10.1016/j.earscirev.2018.05.010

Garzanti, E., Ando, S., & Vezzoli, G. (2006). The continental crust as a source of sand (southern Alps cross section, northern Italy). *The Journal of Geology*, *114*(5), 533–554. https://doi.org/10.1086/506159

Garzanti, E., Dinis, P., Vermeesch, P., Andò, S., Hahn, A., Huvi, J., Limonta, M., Padoan, M., Resentini, A., Rittner, M., & Vezzoli, G. (2018). Dynamic uplift, recycling, and climate control on the petrology of passive-margin sand (Angola). *Sedimentary Geology*, *375*, 86–104. https://doi.org/10.1016/j.sedgeo.2017.12.009

Garzanti, E., Doglioni, C., Vezzoli, G., & Ando, S. (2007). Orogenic belts and orogenic sediment provenance. *The Journal of Geology*, *115*(3), 315–334. https://doi.org/10.1086/512755

Garzanti, E., Vermeesch, P., Andò, S., Vezzoli, G., Valagussa, M., Allen, K., Kadi, K. A., & Al-Juboury, A. I. (2013). Provenance and recycling of Arabian desert sand. *Earth-Science Reviews*, *120*, 1–19. https://doi.org/10.1016/j.earscirev.2013.01.005

Garzanti, E., Vermeesch, P., Padoan, M., Resentini, A., Vezzoli, G., & Andò, S. (2014). Provenance of passive-margin sand (Southern Africa). *The Journal of Geology*, *122*(1), 17–42. https://doi.org/10.1086/674803

Gazzi, P. (1966). Le arenarie del flysch sopracretaceo dell'Appennino modenese; Correlazioni coni flysch di Monghidoro. *Minerelogica et Petrographica Acta*, *12*, 69–97.

Gehrels, G., Giesler, D., Olsen, P., Kent, D., Marsh, A., Parker, W., Rasmussen, C., Mundil, R., Irmis, R., Geissman, J., & Lepre,

13652117, 2024, 3, Downloaded from https://onlinelibrary.wiley.com/doi/10.1111/bre.12877 by South African Medical Research, Wiley Online Library on [14/06/2024]. See the Terms and Conditions (https://onlinelibrary.wiley.com/terms-and-conditions) on Wiley Online Library for rules of use; OA articles are governed by the applicable Creative Commons License

C. (2020). LA-ICPMS U–Pb geochronology of detrital zircon grains from the Coconino, Moenkopi, and Chinle formations in the Petrified Forest National Park (Arizona). *Geochronology*, *2*(2), 257–282. https://doi.org/10.5194/gchron-2-257-2020

Hanson, E. K., Moore, J. M., Bordy, E. M., Marsh, J. S., Howarth, G., & Robey, J. V. A. (2009). Cretaceous erosion in central South Africa: Evidence from upper-crustal xenoliths in kimberlite diatremes. *South African Journal of Geology*, *112*(2), 125–140.

Hasiotis, S. T., Chan, M. A., & Parrish, J. T. (2021). Defining bounding surfaces within and between eolian and non-eolian deposits, Lower Jurassic Navajo Sandstone, Moab Area, Utah, USA: Implications for subdividing erg system strata. *Journal of Sedimentary Research*, *91*(12), 1275–1304.

Haughton, P. D. W., Todd, S. P., & Morton, A. C. (1991). Sedimentary provenance studies. *Geological Society, London, Special Publications*, *57*, 1–11.

Haughton, S. H. (1924). The Fauna and stratigraphy of the Stormberg Series. *Annals of the South African Museum*, *8*, 1–517.

Head, H. V. (2022). The Karoo sand sea in changing climates: Early Jurassic interdune lakes and erg dynamics in southern Africa. Unpublished PhD thesis (205 pp.). University of Cape Town http://hdl.handle.net/11427/36918

Head, H. V., & Bordy, E. M. (2023a). Lake dynamics in an early Jurassic desert: Evidence from the Clarens formation in southern Africa. *Sedimentology*, *70*(3), 865–894. https://doi.org/10.1111/sed.13066

Head, H. V., & Bordy, E. M. (2023b). Loess or lake sediments: Resolving the origin of massive beds in the lower Jurassic of southern Africa. *Geological Journal*, *58*(5), 1822–1843. https://doi.org/10.1002/gj.4695

Herriott, T. M., Crowley, J. L., Schmitz, M. D., Wartes, M. A., & Gillis, R. J. (2019). Exploring the law of detrital zircon: LA-ICP-MS and CA-TIMS geochronology of Jurassic forearc strata, Cook Inlet, Alaska, USA. *Geology*, *47*(11), 1044–1048. https://doi.org/10.1130/G46312.1

Hofmann, M., Linnemann, U., Hoffmann, K. H., Gerdes, A., Eckelmann, K., & Gärtner, A. (2014). The Namuskluft and Dreigratberg sections in southern Namibia (Kalahari craton, Gariep Belt): A geological history of Neoproterozoic rifting and recycling of cratonic crust during the dispersal of Rodinia until the amalgamation of Gondwana. *International Journal of Earth Sciences*, *103*(5), 1187–1202. https://doi.org/10.1007/s00531-013-0949-6

Holzförster, F., Stollhofen, H., & Stanistreet, I. G. (1999). Lithostratigraphy and depositional environments in the Waterberg-Erongo area, central Namibia, and correlation with the main Karoo Basin, South Africa. *Journal of African Earth Sciences*, *29*(1), 105–123. https://doi.org/10.1016/S0899-5362(99)00083-4

Ingersoll, R. V., Bullard, T. F., Ford, R. L., Grimm, J. P., Pickle, J. D., & Sares, S. W. (1984). The effect of grain size on detrital modes: A test of the Gazzi-Dickinson point-counting method. *Journal of Sedimentary Research*, *54*(1), 103–116. https://doi.org/10.1306/212F83B9-2B24-11D7-8648000102C1865D

Jacobs, J., Pisarevsky, S., Thomas, R. J., & Becker, T. (2008). The Kalahari Craton during the assembly and dispersal of Rodinia. *Precambrian Research*, *160*(1–2), 142–158. https://doi.org/10.1016/j.precamres.2007.04.022

Jay, A. E., Marsh, J. S., Fluteau, F., & Courtillot, V. (2018). Emplacement of inflated P¯ahoehoe flows in the Naude's Nek pass, Lesotho remnant, Karoo continental flood basalt province: Use of flow-lobe tumuli in understanding flood basalt emplacement. *Bulletin of Volcanology*, *80*, 1–16. https://doi.org/10.1007/s00445-017-1189-6

Johnson, M. R. (1976). Stratigraphy and sedimentology of the cape and Karoo sequences in the eastern Cape Province. Unpublished doctoral thesis, Rhodes University, Grahamstown, South Africa, 336 pp. http://hdl.handle.net/10962/d1005617

Johnsson, M. J., & Basu, A. (1993). *Processes controlling the composition of clastic sediments. GSA Special Paper 284*. Geological Society of America.

Johnsson, M. R., Anhaeusser, C. R., & Thomas, R. J. (2006). *The geology of South Africa* (p. 691). Geologicla Society of South Africa and Council for Geoscience.

Jordan, T. A., Riley, T. R., & Siddoway, C. S. (2020). The geological history and evolution of West Antarctica. *Nature Reviews Earth and Environment*, *1*(2), 117–133. https://doi.org/10.1038/s43017-019-0013-6

Knoll, F. (2005). The tetrapod fauna of the upper Elliot and Clarens formations in the main Karoo Basin (South Africa and Lesotho). *Bulletin de la Société géologique de France*, *176*(1), 81–91. https://doi.org/10.2113/176.1.81

Kocurek, G., & Dott, R. H., Jr. (1983). Jurassic paleogeography and paleoclimate of the central and southern Rocky Mountains region. *Mesozoic Paleogeography of the West-Central United States: Rocky Mountain Symposium*, *2*, 101–116.

Koen, G. M. (1955). Heavy minerals as an aid to the correlation of sediments of the Karroo system in the northern part of the Union of South Africa. *South African Journal of Geology*, *58*(1), 265–366.

Konopásek, J., Hoffmann, K. H., Sláma, J., & Košler, J. (2017). The onset of flysch sedimentation in the Kaoko Belt (NW Namibia)—Implications for the pre-collisional evolution of the Kaoko–Dom Feliciano–Gariep orogen. *Precambrian Research*, *298*, 220–234.

Kortyna, C., Stockli, D. F., Lawton, T. F., Covault, J. A., & Sharman, G. R. (2023). Impact of Mexican Border rift structural inheritance on Laramide rivers of the Tornillo basin, west Texas (USA): Insights from detrital zircon provenance. *Geosphere*, *19*(6), 1747–1787.

Krynine, P. D. (1948). The megascopic study and field classification of sedimentary rocks. *The Journal of Geology*, *56*(2), 130–165.

Linol, B., de Wit, M. J., Barton, E., de Wit, M. M. J., & Guillocheau, F. (2016). U–Pb detrital zircon dates and source provenance analysis of phanerozoic sequences of The Congo Basin, central Gondwana. *Gondwana Research*, *29*(1), 208–219. https://doi.org/10.1016/j.gr.2014.11.009

Loope, D. B., Steiner, M. B., Rowe, C. M., & Lancaster, N. (2004). Tropical westerlies over Pangaean sand seas. *Sedimentology*, *51*(2), 315–322.

Macey, P. H., Thomas, R. J., Minnaar, H. M., Gresse, P. G., Lambert, C. W., Groenewald, C. A., Miller, J. A., Indongo, J., Angombe, M., Shifotoka, G., Frei, D., Diener, J. F. A., Kisters, A. F. M., Dhansay, T., Smith, H., Doggart, S., Le Roux, P., Hartnady, M. I., & Tinguely, C. (2017). Origin and evolution of the ~1.9Ga Richtersveld magmatic arc, southwest Africa. *Precambrian Research*, *292*, 417–451. https://doi.org/10.1016/j.precamres.2017.01.013

Marsh, J. S., Hooper, P. R., Rehacek, J., Duncan, R. A., & Duncan, A. R. (1997). Stratigraphy and age of Karoo basalts of Lesotho and

13652117, 2024, 3, Downloaded from https://onlinelibrary.wiley.com/doi/10.1111/bre.12877 by South African Medical Research, Wiley Online Library on [14/06/2024]. See the Terms and Conditions (https://onlinelibrary.wiley.com/terms-and-conditions) on Wiley Online Library for rules of use; OA articles are governed by the applicable Creative Commons License

implications for correlations within the Karoo igneous province. *Geophysical Monograph Series*, *100*, 247–272.

McPhee, B., Bordy, E. M., Sciscio, L., & Choiniere, J. (2017). The sauropodomorph biostratigraphy of the Elliot formation of southern Africa: Tracking the evolution of Sauropodomorpha across the Triassic–Jurassic boundary. *Acta Palaeontologica Polonica*, *62*(3), 441–465.

Milliken, K. L. (1988). Loss of provenance information through subsurface diagenesis in Plio-Pleistocene sandstones, northern Gulf of Mexico. *Journal of Sedimentary Research*, *58*, 992–1002.

Minnaar, H. (2011). Composition and evolution of the Proterozoic Vioolsdrif batholith (including the Orange River Group), Northern Cape Province, South Africa. Unpublished doctoral thesis, University of the Free State, p. 184 http://hdl.handle.net/11660/2169

Morton, A. C. (1984). Stability of detrital heavy minerals in Tertiary sandstones from the North Sea Basin. *Clay Minerals*, *19*, 287–308.

Morton, A. C. (1985). Heavy minerals in provenance studies. *Provenance of Arenites*, NATO ASI Series 148, 249–277.

Morton, A. C., & Hallsworth, C. (2007). Stability of detrital heavy minerals during burial diagenesis. *Developments in Sedimentology*, *58*, 215–245. https://doi.org/10.1016/S0070-4571(07)58007-6

Moulin, M., Fluteau, F., Courtillot, V., Marsh, J., Delpech, G., Quidelleur, X., & Gérard, M. (2017). Eruptive history of the Karoo lava flows and their impact on Early Jurassic environmental change. *Journal of Geophysical Research: Solid Earth*, *122*(2), 738–772. https://doi.org/10.1002/2016JB013354

Moulin, M., Fluteau, F., Courtillot, V., Marsh, J., Delpech, G., Quidelleur, X., Gérard, M., & Jay, A. E. (2011). An attempt to constrain the age, duration, and eruptive history of the Karoo flood basalt: Naudes Nek section (South Africa). *Journal of Geophysical Research: Solid Earth*, *116*(B7), 1–27. https://doi.org/10.1029/2011JB008210

Muhs, D. R. (2004). Mineralogical maturity in dune fields of North America, Africa and Australia. *Geomorphology*, *59*(1–4), 247–269. https://doi.org/10.1016/j.geomorph.2003.07.020

Muir, R. A., Bordy, E. M., Mundil, R., & Frei, D. (2020). Recalibrating the breakup history of SW Gondwana: U–Pb radio-isotopic age constraints from the southern Cape of South Africa. *Gondwana Research*, *84*, 177–193. https://doi.org/10.1016/j.gr.2020.02.011

Nxumalo, V. (2020). Uranium mineralisation and provenance analyses of the Karoo Supergroup in the Springbok Flats coalfield, South Africa. Unpublished doctoral thesis, University of Johannesburg.

Pankhurst, R. J., Leat, P. T., Sruoga, P., Rapela, C. W., Márquez, M., Storey, B. C., & Riley, T. R. (1998). The Chon Aike province of Patagonia and related rocks in West Antarctica: A silicic large igneous province. *Journal of Volcanology and Geothermal Research*, *81*(1–2), 113–136.

Pankhurst, R. J., Rapela, C. W., Fanning, C. M., & Márquez, M. (2006). Gondwanide continental collision and the origin of Patagonia. *Earth-Science Reviews*, *76*(3–4), 235–257. https://doi.org/10.1016/j.earscirev.2006.02.001

Pankhurst, R. J., Riley, T. R., Fanning, C. M., & Kelley, S. P. (2000). Episodic silicic volcanism in Patagonia and the Antarctic Peninsula: Chronology of magmatism associated with the break-up of Gondwana. *Journal of Petrology*, *41*(5), 605–625. https://doi.org/10.1093/petrology/41.5.605

Paton, C., Hellstrom, J., Paul, B., Woodhead, J., & Hergt, J. (2011). Iolite: Freeware for the visualisation and processing of mass spectrometric data. *Journal of Analytical Atomic Spectrometry*, *26*(12), 2508–2518.

Paton, C., Woodhead, J. D., Hellstrom, J. C., Hergt, J. M., Greig, A., & Maas, R. (2010). Improved laser ablation U-Pb zircon geochronology through robust downhole fractionation correction. *Geochemistry, Geophysics, Geosystems*, *11*(3), QOAA06.

Petrus, J. A., & Kamber, B. S. (2012). VizualAge: A novel approach to laser ablation ICP-MS U-Pb geochronology data reduction. *Geostandards and Geoanalytical Research*, *36*(3), 247–270. https://doi.org/10.1111/j.1751-908X.2012.00158.x

Pinto, V. M., Hartmann, L. A., Santos, J. O., & Mcnaughton, N. J. (2015). Zircon ages delimit the provenance of a sand extrudite from the Botucatu formation in the Paraná volcanic province, Iraí, Brazil. *Anais da Academia Brasileira de Ciências*, *87*, 1611–1622.

Pol, D., Ramezani, J., Gomez, K., Carballido, J. L., Carabajal, A. P., Rauhut, O. W. M., Escapa, I. H., & Cúneo, N. R. (2020). Extinction of herbivorous dinosaurs linked to Early Jurassic global warming event. *Proceedings of the Royal Society B*, *287*(1939), 20202310. https://doi.org/10.1098/rspb.2020.2310

Rademan, Z. (2018). Radiometric dating and stratigraphic reassessment of the Elliot and Clarens formations; near Maphutseng and Moyeni, Kingdom of Lesotho, Southern Africa. Unpublished Masters thesis, Stellenbosch University.

Rapela, C. W., Pankhurst, R. J., Casquet, C., Baldo, E., Galindo, C., Fanning, C. M., & Dahlquist, J. M. (2010). The Western Sierras Pampeanas: Protracted Grenville-age history (1330–1030 Ma) of intra-oceanic arcs, subduction–accretion at continental-edge and AMCG intraplate magmatism. *Journal of South American Earth Sciences*, *29*(1), 105–127. https://doi.org/10.1016/j.jsames.2009.08.004

Rino, S., Kon, Y., Sato, W., Maruyama, S., Santosh, M., & Zhao, D. (2008). The Grenvillian and Pan-African orogens: world's largest orogenies through geologic time, and their implications on the origin of superplume. *Gondwana Research*, *14*(1–2), 51–72. https://doi.org/10.1016/j.gr.2008.01.001

Rodríguez-López, J. P., Clemmensen, L. B., Lancaster, N., Mountney, N. P., & Veiga, G. D. (2014). Archean to Recent aeolian sand systems and their sedimentary record: current understanding and future prospects. *Sedimentology*, *61*(6), 1487–1534.

Rust, I. C. (1967). On the sedimentation of the Table Mountain Group in the western Cape Province (Doctoral dissertation, Stellenbosch: Stellenbosch University).

Ryan, P. J., & Whitfield, G. G. (1979). Basinal analysis of the Ecca and lowermost Beaufort beds and associated coal, uranium and heavy mineral beach sand occurrences. In some sedimentary basins and associated ore deposits of South Africa. *Special Publication Geological Society of South Africa*, *6*, 91–101.

Scherer, C. M., & Goldberg, K. (2010). Cyclic cross-bedding in the eolian dunes of the Sergi Formation (Upper Jurassic), Recôncavo Basin: Inferences about the wind regime. *Palaeogeography, Palaeoclimatology, Palaeoecology*, *296*(1-2), 103–110.

Scherer, C. M., & Lavina, E. L. (2005). Sedimentary cycles and facies architecture of aeolian–fluvial strata of the Upper Jurassic Guará Formation, Southern Brazil. *Sedimentology*, *52*(6), 1323–1341.

Scherer, C. M., Lavina, E. L., Dias Filho, D. C., Oliveira, F. M., Bongiolo, D. E., & Aguiar, E. S. (2007). Stratigraphy and facies

13652117, 2024, 3, Downloaded from https://onlinelibrary.wiley.com/doi/10.1111/bre.12877 by South African Medical Research, Wiley Online Library on [14/06/2024]. See the Terms and Conditions (https://onlinelibrary.wiley.com/terms-and-conditions) on Wiley Online Library for rules of use; OA articles are governed by the applicable Creative Commons License

architecture of the fluvial–aeolian–lacustrine Sergi Formation (Upper Jurassic), Recôncavo Basin, Brazil. *Sedimentary Geology*, *194*(3-4), 169–193.

Schneider, S., Hornung, J., Hinderer, M., & Garzanti, E. (2016). Petrography and geochemistry of modern river sediments in an equatorial environment (Rwenzori Mountains and Albertine rift, Uganda)—Implications for weathering and provenance. *Sedimentary Geology*, *336*, 106–119. https://doi.org/10.1016/j.sedgeo.2016.02.006

Schwartz, T. M., Souders, A. K., Lundstern, J. E., Gilmer, A. K., & Thompson, R. A. (2023). Revised age and regional correlations of Cenozoic strata on Bat Mountain, Death Valley region, California, USA, from zircon U-Pb geochronology of sandstones and ash-fall tuffs. *Geosphere*, *19*(1), 235–257. https://doi.org/10.1130/GES02543.1

Scotese, C. R. (2014). Atlas of Jurassic paleogeographic maps (Mollweide projection), map 45, volume 4 of the PALEOMAP atlas for ArcGIS, PALEOMAP Project, Evanston, IL.

Sharman, G. R., & Malkowski, M. A. (2020). Needles in a haystack: Detrital zircon U-Pb ages and the maximum depositional age of modern global sediment. *Earth-Science Reviews*, *203*, 103109.

Smith, R. M. H., Eriksson, P. G., & Botha, W. J. (1993). A review of the stratigraphy and sedimentary environments of the Karoo-aged basins of Southern Africa. *Journal of African Earth Sciences*, *16*(1–2), 143–169.

Stagman, J. G. (1978). An outline of the geology of Rhodesia with contributions from N.M. Harrison, T.J. Broderick and V.R. Stocklmayer. *Bulletin—Geological Survey of Rhodesia*, *80*, 126.

Stockley, G. M. (1947). *Report on the geology of Basutoland* (p. 114). Morija Printing Works.

Svensen, H., Bebout, G., Kronz, A., Li, L., Planke, S., Chevallier, L., & Jamtveit, B. (2008). Nitrogen geochemistry as a tracer of fluid flow in a hydrothermal vent complex in the Karoo Basin, South Africa. *Geochimica et Cosmochimica Acta*, *72*, 4929–4947. https://doi.org/10.1016/j.gca.2008.07.023

Svensen, H., Corfu, F., Polteau, S., Hammer, Ø., & Planke, S. (2012). Rapid magma emplacement in the Karoo large Igneous Province. *Earth and Planetary Science Letters*, *325–326*, 1–9. https://doi.org/10.1016/j.epsl.2012.01.015

Svensen, H., Jamtveit, B., Planke, S., & Chevallier, L. (2006). Structure and evolution of hydrothermal vent complexes in the Karoo Basin, South Africa. *Journal of the Geological Society*, *163*, 671–682. https://doi.org/10.1144/1144-764905-037

Thompson, A. O. (1975). The Karoo Rocks in the Mazunga Area, Beitbridge District. *Short Report, Geological Survey of Rhodesia*, *40*, 79.

Van Dijk, D. E., & Eriksson, P. G. (2021). Bipedal leaping Jurassic vertebrates in Southern Africa: Proposed new ichnotaxon and inferred palaeoenvironment. *Transactions of the Royal Society of South Africa*, *76*(3), 235–245. https://doi.org/10.1080/00359 19X.2021.1964104

Van Kranendonk, M. J., & Kirkland, C. L. (2013). Orogenic climax of earth: The 1.2–1.1 Ga Grenvillian superevent. *Geology*, *41*(7), 735–738.

Van Niekerk, H. S. (2006). The origin of the Kheis terrane and its relationship with the Archean Kaapvaal Craton and the Grenvillian Namaqua Province in southern Africa. Unpublished doctoral thesis, University of Johannesburg.

Vermeesch, P. (2018). IsoplotR: A free and open toolbox for geochronology. *Geoscience Frontiers*, *9*(5), 1479–1493. https://doi.org/10.1016/j.gsf.2018.04.001

Viglietti, P. A., Frei, D., Rubidge, B. S., & Smith, R. M. (2018). U-Pb detrital zircon dates and provenance data from the Beaufort Group (Karoo Supergroup) reflect sedimentary recycling and air-fall tuff deposition in the Permo-Triassic Karoo foreland basin. *Journal of African Earth Science*, *143*, 59–66. https://doi.org/10.1016/j.jafrearsci.2017.11.006

Viglietti, P. A., McPhee, B. W., Bordy, E. M., Sciscio, L., Barrett, P. M., Benson, R. B. J., Wills, S., Chapelle, K. E. J., Dollman, K. N., Mdekazi, C., & Choiniere, J. N. (2020). Biostratigraphy of the Massospondylus assemblage zone (Stormberg group, Karoo supergroup), South Africa. *South African Journal of Geology*, *123*, 249–262. https://doi.org/10.25131/sajg.123.0018

Visser, J. N. J. (1984). A review of the Stormberg group and Drakensberg volcanics in southern Africa. *Palaeontologia Africana*, *25*, 5–27.

Vorster, C. (2014). Laser ablation ICP-MS age determination of detrital zircon populations in the phanerozoic cape and Lower Karoo Supergroups (South Africa) and correlatives in Argentina. Unpublished doctoral thesis, University of Johannesburg.

Weltje, G. J., & von Eynatten, H. (2004). Quantitative provenance analysis of sediments: Review and outlook. *Sedimentary Geology*, *171*(1–4): 1–11. https://doi.org/10.1016/j.sedgeo.2004.05.007

Zieger, J., Harazim, S., Hofmann, M., Gärtner, A., Gerdes, A., Marko, L., & Linnemann, U. (2020). Mesozoic deposits of SW Gondwana (Namibia): Unravelling Gondwanan sedimentary dispersion drivers by detrital zircon. *International Journal of Earth Sciences*, *109*(5), 1683–1704. https://doi.org/10.1007/s00531-020-01864-2

SUPPORTING INFORMATION

Additional supporting information can be found online in the Supporting Information section at the end of this article.

How to cite this article: Head, H. V., Bordy, E. M., & Bolhar, R. (2024). Sedimentation tempo in an Early Jurassic erg system: Refined chronostratigraphy and provenance of the Clarens Formation of southern Africa. *Basin Research*, *36*, e12877. https://doi.org/10.1111/bre.12877

13652117, 2024, 3, Downloaded from https://onlinelibrary.wiley.com/doi/10.1111/bre.12877 by South African Medical Research, Wiley Online Library on [14/06/2024]. See the Terms and Conditions (https://onlinelibrary.wiley.com/terms-and-conditions) on Wiley Online Library for rules of use; OA articles are governed by the applicable Creative Commons License